

ASSESSMENT OF LULC AND LST OF ISLAMABAD AND RAWALPINDI, PAKISTAN, USING GEO-SPATIAL TECHNIQUES



By

AFIFA KANWAL

AIMEN ANSAR

EHSIN ATHER

Department of Earth and Environmental Sciences

Bahria University, Islamabad, Pakistan

2018-2022

Dedication

We dedicate our thesis, wholeheartedly, to our parents who worked day and night for us to be able to attain knowledge in a prestigious university, for always being there for us, for providing us with such a blissful lifestyle, for financially supporting us, and for giving up strength, encouragement, and inspiration to complete this thesis.

Abstract

The rapid urbanization and population growth over the past three to four decades has caused a change in the Land use and land cover patterns in the twin cities of Pakistan (Islamabad and Rawalpindi). This in turn has led to a change in land surface temperatures. The knowledge of various man-made phenomena on the surface of the earth is improved through the study of Land Use and Land Cover (LULC) changes and their patterns. As Pakistan is in the top ten countries that are going to be affected by climate change, thus there is an urgent need to monitor the environment to make better decisions. The area of interest in this study is the city of Islamabad (33.7205° N, 73.0405° E) and Rawalpindi (33.5651° N, 73.0169° E). The area was selected for the study because it has seen drastic changes since the start of the 21st century. The time period of 4 decades was taken, from 1990 to 2021, and calculations were done after every decade. The satellite imagery of the study area was taken from the United States Geographical Survey (USGS) for each decade. LANDSAT 4-5 imagery was used for the year 1990 to 2010 and for the year 2021 LANDSAT 8 imagery was used. The study focuses on changes in the Land Cover Changes and also how these changes correspond with the changes in the temperature over the years. Land Use and Land Cover were analyzed by a supervised classification system. For Land Surface Temperature, Thermal, Red, and Infra-Red bands were used to calculate the changes in temperature. The results of Land Cover changes were found, and the maximum change was observed in urbanization followed by barren, vegetation, water, and then forest. A trend of decreasing lower temperature and increasing higher temperature was observed, where net changes of 13.72, and 11.81 in degree centigrade were analyzed respectively. These changes are crucial for any urban city development and for climate change study, and they also provide baseline information for decisions and policymakers.

Acknowledgment

First and foremost, we would like to thank the Al-Alim, the All-Knowing, Allah Al-Mighty for giving us this chance and opportunity, the knowledge, and the skills to be able to conduct this thesis.

We would like to express our deepest gratitude to our teacher and supervisor, Dr. Humera Farah, without whom this thesis would not be possible. She is a role model, an excellent teacher, and an exceptional superintendent, who throughout the course of our thesis, provided us with guidance, encouragement, and assistance.

We are immensely grateful to Engr Sher Shah from Global Climate Impact Studies Center (GCISC) for his exceptionally thorough assistance, engaging us with concepts, theories, and ideas of everything related to our thesis subject, and for giving us guidance even with his busy schedule.

We also appreciate and acknowledge our Head of Department, Dr. Said Akbar Khan, and the faculty of the Earth and Environmental Sciences Department at Bahria University, Islamabad, for providing us with this opportunity to conduct this thesis.

We feel forever in debt and grateful to Mr. Arif Rashid Goheer (Head Agriculture & Coordination/Director Admin) Global Climate Impact Studies Center (GCISC) for accepting us and providing us with the opportunity to conduct our thesis in their department.

Contents

Chapter 1 - Introduction	1
1.0. General overview.....	1
1.1. Urbanization.....	1
1.2. Causes of Urbanization	2
1.2.1. Deforestation	3
1.2.2. Barren land/desertification.....	5
1.2.3. Agriculture	7
1.2.4. Freshwater	9
1.3. Land Use and Land Cover (LULC).....	13
1.4. Significance of Land Use and Land Cover (LULC)	15
1.4.1. Mapping urban areas:	15
1.4.2. Urban expansion:	16
1.4.3. Agriculture land:	17
1.4.4. Forest area:	17
1.5. Land Surface Temperature (LST).....	18
1.6. Significance of Land Surface Temperature (LST).....	19
1.7. Geographical Information System (GIS) & Remote Sensing (RS).....	20
1.7.1. ArcGIS software	21
1.7.2. Remote sensing.....	22
1.8. Role of GIS & remote sensing in LULC & LST	23
1.8.1. Mapping:	24
1.8.2. Study of reactions and outcomes:	24
1.8.3. Impact evaluation:	25
1.8.4. Urban development:	25

1.9. Land-use Satellite (LANDSAT)	25
1.9.1. Landsat 8.....	25
1.9.2. Landsat 4-5.....	26
1.10. Problem statement.....	27
1.11. Objectives	27
Chapter 2 - Literature review	29
2.1. Literature Review.....	29
2.2. Rationale of the study.....	36
Chapter 3 - Materials and methods	39
3.1. Study area.....	39
3.2. Materials and methods.....	40
3.2.1. Satellite imagery data acquisition	40
3.2.2. Image Processing of Land use and Land Cover (LULC)	40
3.2.3. Image classification.....	42
3.3. Image Processing for Land Surface Temperature (LST)	45
3.3.1. Top Of the Atmosphere calculation (TOA)	46
3.3.2. Brightness Temperature calculation (BT)	46
3.3.3. Normalized Differential Vegetation Index (NDVI) calculation.....	48
3.3.4. Proportion of Vegetation calculation (PV).....	48
3.3.5. Emissivity calculation (ϵ)	49
3.3.6. LST calculation	49
3.4. Accuracy assessment	50
3.4.1. Marking of reference points on Google Earth pro	50
3.4.2. Sequencing of Earth pro points and ArcGIS points.....	51
3.4.3. Extract value to points.....	51

3.4.4. Frequency table.....	52
3.4.5. Error matrix.....	52
3.4.6. Accuracy assessment final table	52
Chapter 4 - Result and Discussion	54
4.1. Study area's parameters description	54
4.1.1. Geology and general topography	54
4.1.2. Population trend	55
4.1.3. Hydrology.....	55
4.1.4. General climate	56
4.2. Pattern of Land Use and Land Cover Changes (LULC)	56
4.2.1. 1990.....	56
4.2.2. 2000.....	58
4.2.3. 2010.....	59
4.2.4. 2021.....	61
4.2.5. Decade-wise LULC area for each class	63
4.3. Net change in LULC.....	64
4.4. Accuracy assessment	65
4.5. Accuracy assessment points	65
4.6. Pattern of Land Surface Temperature (LST) changes	66
4.6.1. 1990.....	66
4.6.2. 2000.....	68
4.6.3. 2010.....	69
4.6.4. 2021.....	70
4.7. Net Change in LST.....	72
4.8. Comparison with other studies.	74

Chapter 5 – Conclusion and Recommendation	76
5.1. Conclusion	76
5.2. Recommendations	76
References.	78
Appendices	86

Table of Figures

Figure 3.1: Study Area Map.....	39
Figure 3.2: Methodology of LULC.....	45
Figure 3.3: Methodology of LST	50
Figure 4.4: LULC 1990.....	58
Figure 4.5: LULC 2000.....	59
Figure 4.6: LULC 2010.....	61
Figure 4.7: LULC 2021.....	63
Figure 4.8: Assessment points of year 1990	66
Figure 4.9: Assessment points of year 2000	66
Figure 4.10: Assessment points of year 2010	66
Figure 4.11: Assessment points of year 2021	66
Figure 4.12: LST 1990	67
Figure 4.13: LST 2000	69
Figure 4.14: LST 2010	70
Figure 4.15: LST 2021	72

Table of tables

Table 2.1: Literature review table	35
Table 3.2: Satellite imagery data acquisition.....	40
Table 3.3: Bands combination of LANDSAT 4-5, and LANDSAT 8.....	43
Table 3.4: The five Classifications	43
Table 4.5: LULC area per decade.....	63
Table 4.6: Net changes in LULC.....	65
Table 4.7: Accuracy assessment of Land Use and Land Cover	65
Table 4.8: LST 2000 (low, high, and net changes in temperature)	68
Table 4.9: LST 2010 (Low, high, and net change in temperature)	70
Table 4.10: LST 2021 (low, high, and net changes in temperature)	71
Table 4.11: LST net changes in area km² and area Percentage.....	72
Table 4.12: Net changes in LST (degree Centigrade).....	73

Abbreviations

LULC: Land Use Land Cover	GDP: Gross Domestic Product
LST: Land Surface Temperature	NWFP: North-West Frontier Province
GIS: Geographic Information System	IGBP: International Geosphere-Biosphere Programme
TOA: Top Of the Atmosphere	IHDP: International Human Dimensions Programme
BT: Brightness Temperature	TIR: Thermal InfraRed
NDVI: Normalized difference vegetation index	RTE: Radiative Transfer Equation
PV: Proportion of Vegetation	BIM: Building Information Modeling
UN: United Nations	CAD: Computer-Aided Design
WWF: World Wide Fund for Nature	PCA: Principal Component Analysis
FAO: Food and Agriculture Organization	ANN: Artificial Neural Network
UNEP: United Nations Environment Programme	LANDSAT: Land Satellite
CBD: Convention on Biological Diversity	LDCM: Linear Dimming Control Module
UNFCCC: United Nations Framework Convention on Climate Change	USS: Ultra Sonic Sensor
KPK: Khyber Pakhtunkhwa	OLI: Operational Land Imager
IR: Infra-Red	EO: Electro-optical
DOI: Digital Object Identifier	USGS: United States Geological Survey
NASA: National Aeronautics and Space Administration	SSR: Solid State Recorders
WRS: Worldwide Reference System	MSS: Multispectral Scanner

NOAA: National Oceanic and Atmospheric Administration	EOSAT: Earth Observation Satellite Company
TDRSS: U.S. Tracking And Data Relay Satellite	TM: Thematic Mapper
GE: General Electrics	LDVI: Land Degradation Vulnerability Index)
GMP: Gamma Irradiator Service	MODIS: Moderate Resolution Imaging Spectroradiometer
AHP: Analytic Hierarchy Process	NDBI: Normalized Difference Built-Up Index
CPEC: China–Pakistan Economic Corridor	RLST: Relative Land Surface Temperature
AOI: Area of Interest	TIFF: Tag Image File Format
PNG: Portable Network Graphic	JPEG: Joint Photographic Experts Group
M_L: Radiance Multiplier Band	A_L: Radiance Additive Band
DN: Digital Number	KML: Keyhole Markup Language

Chapter 1 - Introduction

1.0. General overview

As of October 2011, the global population has increased to 7 billion people and is rapidly increasing (Li, Liu, and Sang, 2012). It is projected that the population will grow up to 10.9 billion people at the end of this century, from 7.7 billion people current population (Maja and Ayano, 2021). It is projected that regions of low-income and poor countries, with population dependent on nature, is seeing more growth than other regions. These regions include Sub-Saharan Africa and the Southeast Asian region with an annual population growth of 2.5% (United Nations, 2019). These regions are undergoing sudden and rapid economic and demographic changes, “demographic transition”, which is why they are in a rapid population growth phase (Bongaarts and Casterline, 2013). According to a projection done by the UN, more than half of global population change will be brought from the population change in Sub-Saharan Africa and the Southeast Asian region (Maja and Ayano, 2021). The change in Sub-Saharan Africa in terms of fertility is more than in the Central, Southeast Asian regions, and Western Asia by about 4.6 live births per woman in Sub-Saharan Africa (DESA, 2019). These areas are expected to increase the global population increase by half a billion people in the upcoming three decades, despite having a declining birth rate, and about 25% of the total global population will be concentrated in these regions. This rapid increase in population coupled with migration from rural areas to urban areas and fast economic development is causing intense pressure on food, water, energy utilization, and production, all of which in return affect or harm the environment and also contribute to the climate change (Jiang and Hardee 2011; Molotoks et al. 2018; Maja and Ayano, 2021).

1.1. Urbanization

Rural to urban areas migration is increasing at an alarming rate. According to a recent report published by United Nations Population Division, within the upcoming 30 years, the growth of urban areas will increase from about half the population living in urban areas currently to two-thirds living in urban areas. Between the years 2000 and 2030, the global population growth is expected to grow from about 48.3% currently residing in the urban

area (about 2.8 billion people compared to a total of 6.0) to 60.4% living in 2030 (60.4% living in urban areas, about 4.9 billion people of total of 8.1 billion). According to an old study, by 2007, most of the world's population will be living in urban areas. Less wealthy regions will see more (from about a growth of 1.9 billion in 2000 to roughly 3.9 billion in 2030) with the highest growth rate expected to be happening in Asia and Africa. Compared to Asia, North America and Europe are currently more developed urbanized regions, but still, the number of urban people living in those regions (about 1.2 billion) is less than the number of people living in Asia (1.4 billion), already in the year 2000 (Vlahov and Galea, 2002). The United Nations defines a city with a population of over 10, 000, 000 as a megacity (Li, Liu, and Sang, 2012). The pace at which the urban areas are seeing an increase is different in different regions. It is estimated that the proportion of people living in megacities has increased to 5.2% in 2015 from 4.3% in 2000. The rate of growth in underdeveloped countries was much higher than the developed countries. But there will be more increase in small cities' population (cities with a population of less than 5 million), than the large cities by almost 25% more increase in small cities. Thus, there was more population increase in small cities, but the number also increased in the megacities, which undoubtedly, created many challenges in the health and environmental sector (Vlahov and Galea, 2002).

1.2. Causes of Urbanization

Resource depletion and consumption are different in different areas, regions, and countries and the change is substantial between developed and underdeveloped countries. The level of resource consumption is higher in developed countries than the underdeveloped countries as they aspire to have a better and better lifestyle and also depend a lot on resources that contribute to solid waste production. That's why their rate of resource exploitation, regardless of whether it's exploited inside their country or outside, is higher than the underdeveloped nations. In contrast, people in underdeveloped countries are living much more resource-independent life. But this doesn't mean that underdeveloped countries are not moving toward where developed nations are heading. Underdeveloped countries due to lack of education, awareness, increase in population, and also the aspiration to have a more luxurious and better lifestyle are causing a lot of harm and

degradation of the environment. The idea of consumerism and a capitalistic market has prevailed in underdeveloped nations as well. So, in both, the underdeveloped and the developed nations, the current trend of energy, natural resources consumption, agricultural practices, and the rate of urbanization is inclined more toward unsustainable patterns rather than eco-friendly and sustainable ones. If this trend continues, these patterns can lead to many problems like climate change and reduced economic growth due to a decrease in environmental productivity (Mittal and Gupta, 2017). Earth is a planet with a finite number of resources (Maja and Ayano, 2021). The sudden increase in the demand for natural resources, after the industrial revolution, is causing dramatic depletion of these resources particularly in countries that are overly dependent on them (WWF, 2018). Though developed nations are consuming more natural resources, the underdeveloped countries have more natural resources quantitatively but are causing a lot of harm by deforestation, overgrazing, and loss of biodiversity (Toth and Szigeti, 2016; Mittal and Gupta, 2017).

1.2.1. Deforestation

The terms forest and deforestation are known commonly but in science, these terminologies need to be clearly defined first before we talk about them, and this definition must be measurable. There still needs to be a proper single definition of forest that needs to be created and agreed upon by everyone but we still don't have one, even though these terms are a global issue. Let's first study the definition of FAO (Food and Agriculture Organization, which is an established institute). FAO (2006) defines forests as an area of land that is more than 0.5 hectares and has trees higher than 5 meters with a canopy cover of more than 10 percent. But this definition excludes land that doesn't lie under forest area is excluded. Let's see another definition. According to the United Nations Environmental Program/the Convention of Biological Diversity (UNEP/CBD, 2001), it excludes those temporary un-stocked areas (areas that have yet to reach the crown density and height) but all other parameters are the same: i.e., minimum 0.5 hectares, crown over 10 percent and height of trees 5 meters. Lastly, let's see the definition of the United Nations Framework Convention on Climate Change (UNFCCC, 2006). According to UNFCCC, the minimum area needs to be from 0.05 to 1.0 hectares, with a tree canopy of 10 to 30 percent and height from 2 to 5 meters (Indarto et al, 2016).

In Europe, the Middle East, and Asia, deforestation has been called the reason for ecological degradation (Marsh, 1874; von Wissman et al. 1956; Thirgood, 1981; Thomas, 1956). Since the 1970s, the awareness of the severity of the problem of deforestation has been brought to light and its impacts on environmental damage and wood shortages. According to FAO, deforestation was recently only confined to Asia and Africa but now is also a problem in Latin America (FAO and IUNEP, 1982). With the exception of a few countries with anomalously high rates of deforestation, deforestation is suggested to be confined to countries, with forests, near the meridians (Allen and Barnes, 1985). Agriculture plays the most significant part in the contribution of deforestation. But agriculture for food is just as important as forests for the ecosystem, therefore, understanding the conversion of forests and implementing sustainable practices are important to achieve the goals of SDGs (Sustainable Development Goals) (Solis and Montania, 2021).

Pakistan has five provinces, one of which is Khyber Pakhtunkhwa (KPK). KPK is a very important province for Pakistan and is very vulnerable to deforestation and climatic changes due to many climate sensitive sectors. A large portion of the whole forest system of Pakistan lies in KPK and the people of KPK also rely mostly on the forest and agriculture sector. According to an estimate, 40% of Pakistan's forest lies in KPK (Ahmad et al. 2012). But the rate of deforestation in this region is high, which makes it prone and vulnerable to floods, landslides, ice caps melting and loss of biodiversity, etc. An example of climate change and its impact not only on KPK but on Pakistan as well as the flood of 2010. The flood caused around 1767 deaths, loss of houses, and damage to property of around 200,733 people, and a total of 43,659,09 people were affected (Kroonstad, Sheikh, and Vaughn, 2010). All these losses can be traced back to the loss of forests and climate change. Conifer forests (which lie at an altitude of 1000 to 4000 meters) are facing the highest rate of deforestation in areas like Dir, Swat, Manshera, etc. (Ahmad et al, 2012; Tariq and Aziz, 2015).

KPK forests are not the only forest under stress, the Himalayan Mountain ecosystem is also facing such stress because of the rapidly increasing population. This is causing habitat fragmentation and degradation of the forest. The earliest time that can be

tracked for deforestation started during the British Raj in the 1850s when forests were cut down for industrial, infrastructure, and other uses. From 1990 to 2000, the total forest area loss is around 74, 613 ha, and between 2000 to 2010, the total area of forest loss of 95,598 ha. The majority of this deforestation occurred in tribal areas. The second has seen a higher rate of deforestation, mainly in the regions of North Waziristan, Upper Dir, and Bajor. Most of the deforestation occurred between the boundaries at both, the international and national district levels. Regarding the district level deforestation, those areas are now either grassland or have become agricultural land (Qamar et al.,2016).

1.2.2. Barren land/desertification

Desertification can be described as land degradation in arid, semi-arid, and dry sub-humid areas resulting from various reasons like variation in climate and human activities, this definition is from one of the principals of the Conference on Environment and Development of United Nations, the AGENDA 21. The land consists of soil, water, flora, fauna, and other ecological processes that occur within the system, and its degradation means ecological and economical loss by loss in productivity of the soil. Different land use forms have different symptoms of desertification. One of the reasons for damage or degradation of irrigated farmlands is the rise of the water table due to improper drainage and or excess use of irrigation. Waterlogging can also cause salinization and other forms of chemical imbalance or damage to the soil. Soil erosion is another reason for soil degradation, which mainly occurs in rain-fed farmlands, and causes loss of organic matter and essential nutrients, compaction of crust formation, and can also cause invasion of weeds. Meanwhile, in rangelands, the degradation is associated with the reduction in bio-productivity, invasion of nonnative species, soil erosion and poor livestock, etc. (Kassas, Ahmad, and Rozanov, 1991).

Desertification is associated with drylands meanwhile land degradation can occur in both drylands and moist lands. In areas where there is more water expenditure and usage, including evapotranspiration, and less water income like precipitation, that area of land is considered dryland. This is the criteria of aridity. Drylands are classified according to this measure, called the aridity index, and the classification falls into four zones (UNEP, 1992): hyper-arid, arid, semiarid, and dry sub-humid. The hyper-arid areas consist of 978 million

ha area, and are practically rainless, therefore are deserts. The arid and semi-arid regions consist of 1571 million ha area and 2305 million ha area, respectively. These are rangelands and rain-fed farmlands. And finally, the dry subhumid areas have a total area of 1296 million ha. These are more bio-productive than other lands mentioned before. The drylands of the Earth, in percent of total area, contribute to about 41% or 6150 million ha. It is worth mentioning that agriculture and vegetation can even occur in hyper drylands given that there is water available like river Niel in Egypt. All these areas are prone to desertification (Kassas, 1994).

When it comes to Pakistan, we have a serious problem of desertification because Pakistan is predominantly an arid and semi-arid region that depends upon irrigated water and rain. Its major export, from agriculture, is the cotton crop. And surprisingly, this cotton is mostly grown in regions like That and the Cholistan Desert. Pakistan has a total area of 79.61 million ha and out of this 79.61 million ha, 68 million ha of land lies in fragile regions which receive very less rainfall (less than 300mm) of annual rainfall. In Pakistan, one-fourth area of the total area suitable for agriculture is susceptible to wind and water erosion, water logging, flooding, and loss of nutrients and organic matter from erosion. Pakistan receives almost all of its water from the Northern mountainous region, and from these regions, the Tarbela and Mangla dam, which are the largest dams in Pakistan and contributes to 90 percent of the water for food and crop production, are filled with streams coming from Northern areas. But the capacity of dams is decreasing due to silting up and sedimentation. Meanwhile, overgrazing, bad agricultural practices, and heavy soil erosion further leads to more degradation of arid lands. The irrigated lands are now prone and vulnerable to waterlogging and salinity. In the province of Baluchistan, due to the already shortage of annual rainfall and the dependence of the entire province on groundwater for agriculture and horticulture, has dropped the water level dramatically. Rangelands productivity has decreased from livestock pressure. The reduced freshwater flows, sewage, industrial pollution, and over sage of natural usage, are causing tremendous stress on the mangrove forest as well (Babur, Ali, and Baig, 2013).

1.2.3. Agriculture

Agriculture is associated with many facilities and services but all of them come with a price. Agriculture provides us with food, open space, and scenery but on the other hand, agriculture contributes to numerous and enormous environmental problems. One of the biggest contributors to water quality degradation and degradation of aquatic habitats are Nitrates and pesticide runoff. Not only do they degrade the quality of water for drinking purposes, but they also damage the habitat of fishes and other organisms and also cause eutrophication that can affect estuaries, lakes, rivers, and also commercial fisheries. On the other hand, bacteria also contaminate the drinking water and can contaminate the shellfish as well. Usually, these bacteria come from animal waste. The animal waste of livestock can also produce odor in the drinking water and affect the quality of water in residential areas. Erosion and then sedimentation can cause an increase in the cost of water treatment of drinking water and also increases the need for dredging. Exposure from pesticides to farmers can produce both, acute and chronic, illnesses. Meanwhile, pesticide residues adhered to food can prove detrimental to human life and health. Damage from pesticides to the ecosystem includes the death of fishes, birds, and animals and also damage to flora and land as well, including but not limited to, the degradation of forests, wetlands, and grasslands. Other contaminations like heavy metals have huge impacts on the ecosystem, including, the death of wildlife and damage to their reproductive system as well as serious health hazards for human health. The runoff of irrigation water can salinize the crops and the downstream rivers. The runoff can also cause drainage issues in the downstream areas (Lichtenberg, 2002).

There are other ways by which ecosystems can be polluted or degraded, including, urbanization, rapid industrialization, wastes whether organic or inorganic, and bad agricultural practices. Some of the bad agricultural practices include excessive or wrong utilization of pesticides and chemical fertilizers, tillage, and ineffective and unsustainable irrigation. Other bad practices include the burning of post-harvest crop residues, agriculture without rotation, and wrong animal wastes (Gurbuz, 1992). In contrast, the best agricultural techniques are complex to implement and depend upon many factors like weather variability with time and hydrogeological conditions (Zollweg & Makarewicz, 2009).

Decision makers are continuously trying to implement the best agricultural management techniques in order to reduce pollution and degradation all the while helping farmers to have a better yield (Esen and Uslu, 2008). Alongside decision makers, the policymakers also need to consider the local policies and practices and help the farmers to understand and apply the better science and research done in the agriculture sector (Stoate et al., 2009). They also need to inform the farmers about the side effects of synthetic fertilizers and pesticides as their toxicity depends on many factors like temperature, pH, and type of soil (Boxall et al., 2003). These chemicals have the ability to persist in the environment or degrade quickly to have acute effects. Moreover, they can run off to other water bodies or land. For example, fertilizers that have a high amount of Nitrogen in them can cause soil washing, degradation of surface water like lakes, rivers and streams but also degradation of groundwater aquifers as well. The latter, that is groundwater contamination, from chemical fertilizers is a big issue. These chemical fertilizers with a high amount of Nitrogen can break down into nitrates and as they are water soluble, they can seep down into groundwater and can remain there for decades causing an accumulative effect. This Nitrogen, as mentioned before, can also cause Algal Bloom in water, called eutrophication, and can damage the quality of water and cease the growth of other organisms in the water. Even if this Nitrogen is not runoff, it can affect the crops as well, like for example, lettuce and spinach that are grown in a high concentration of Nitrogen can accumulate Nitrogen oxide and Nitrate and also some carcinogenic compounds like Nitrosamine. By standard, drinking water should not contain Nitrogen in amounts of more than 20 parts per million. This is the reason many developed countries have limited the use of nitrogen fertilizers. Lastly, these Nitrogen fertilizers when introduced to the sea, can make “dead zones” in the marine ecosystem. In these dead zones, the nitrogen increases the growth of plant life which ends up using all the dissolved oxygen, and none is left for fishes and other life, which ends up in their death. This is of most importance when that marine ecosystem is the one upon which a community depends (Khan, Ali, and Baig, 2013).

In the context of Pakistan, even though Pakistan is mainly an agricultural country, the crop yield of Pakistan per ha is among the lowest. The major crops grown in Pakistan includes cotton, rice, wheat, sugarcane, and maize. All of these account for 24% of the total value added in the overall agriculture of the country and contributes about 4.67% of the

total GDP. Other minor crops include Bajra, Jowar, and pulses, which have a value of 11.36% of the total agriculture and account for the 2.25% of the GDP. In contrast, the other form of agriculture, that is, livestock, adds 58.55% to the agricultural value and contributes about 11.61% of the GDP. Forestry contributes to about 0.41% of the GDP and adds 2.17% of the agricultural value. And lastly, the fish industry contributes about 0.43% of the GDP and adds 2.17% to the overall agricultural value (Azam and Shifique, 2017).

At the time of its independence, Pakistan's agriculture contributed about 53% of the GDP but slowly fall to about 21%. Thus, from the major three sectors of Pakistan's GDP, the industrial, the agricultural, and commerce; the agricultural sector saw a decline. Now, there are other problems in this sector as well, mainly climate change. Pakistan depends upon its river water and monsoon water for crop production as it is an arid and semi-arid country. Monsoon rain contributes to about 90 to 97% of the total rainwater in the summer season. But as Pakistan did have not enough dams, the year 2010 saw the biggest flood in the country, and the agriculture sector took a huge loss. The total agriculture growth was 1.2% and the total growth of major crops was 4% due to floods. Furthermore, the rapid increase in population is putting stress on the water and energy sectors. The irrigation system may be advanced in the past but now it's too old and requires modernization and improvements. If steps are not taken on time, there is a huge risk of water logging and water salinization (Azam and Shifique, 2017).

1.2.4. Freshwater

Freshwater degradation from pollution and human use has, for the first time in history, a problem where the water shortage will be causing a threat to food security, ecosystem health, and the supply of water to urban areas. The major factor contributing to this is pollution and moreover, the addition of 3 billion more people in the coming decades, will further casing water stress, especially in developing countries. Water pollution and bad water quality is not only affecting humans but other species as well, and that too, on a global scale. Even today, more than one billion people lack an access to clean drinking water and more than two and a half billion people do not have access to their own sanitation and hygienic services. This pollution of water not only causes illnesses, but it is actually the leading cause of death worldwide and is the ground for many waterborne diseases and

diseases from contaminated water. More than 85% of our freshwater is used by the agriculture sector worldwide. Plus, there is a rapid population growth going on, which means there need for more food production. In the coming 5 decades, we will require to increase our food production by 50%, assuming that the already land used for agriculture will not degrade to the point where it can't grow anything anymore, as many factors are playing the role of soil degradation already. But just eating for survival is not enough for human communities, if we were to eliminate poverty and malnutrition, we will have to grow much more than that as there is already an issue of just not food security but also malnutrition in many countries. But for many reasons, the expansion of agricultural lands will only account for a small portion of fulfilling this huge demand, what's more, required at the moment, is the yield per area to be increased. Without proper coordinated planning and help from international cooperation, humans will be facing severe water-related issues which will also affect other life forms as well, but the most affected regions will be the poor regions of the world (Jury and Vaux, 2007).

Another problem related to water is the runoff, globally, of the blue water resources and their accessibility. It is difficult to estimate how much water is runoff and has uncertainties as well (Postel, Gretchen, and Paul, 1996). But the more quoted value is 42, 700 cubic kilometers (Shiklomanov and Mcgranahan, 1997). Some of the reasons why it is hard to estimate the global runoff level is that all regions are not the same. Some regions see more runoff than others. Some regions have an excess amount of surface water while others are facing a severe level of scarcity. In regions where there is an excess amount of water, like Pakistan for example, a much amount of water is runoffs into the ocean without much of it being utilized by society and communities. Another example can be of Amazon River where twenty percent of the total global runoff of water happens, but most of it is not utilized by the local native people (Gleick, 1998). On the other hand, the majority of the Earth's lands see low rainfall annually and are water deficient. Regions by area that are facing the most amount of water shortage are the Middle East, Africa, and some parts of Europe but the population that is and will face the most severe water scarcity per individual is Southeast Asia (Pakistan and India) as their population is huge and is increasing (Jury and Vaux, 2007).

It's only been about 5 decades, since the world at a large scale started to pump groundwater for agricultural and other uses, like municipal, industrial, and urban supplies, by the use of pumps and motors. About 750 to 800 KM³ of fresh water is pumped annually globally per year (Shah et al., 2000). Thus, it is safe to say that using this groundwater had a dramatic advantage for utilization and economic reasons but all of that came with a price. Now, groundwater aquifers are depleting at an alarming rate and the groundwater aquifer level has already gone quite below, which has not only increased the pumping cost by having to drill deeper, the cost of pumping itself has risen too from having to pump more and using more electricity. The groundwater quality is also degrading, the surface water aquatic life has already been damaged by quite some margin and the land is facing irreversible damages in many areas. All of this was inevitable as the rate of groundwater pumping and dependence grew very large. The regions that are mostly affected by it are the Middle East, Central Asia, North Africa, North China, North America, Australia, and other local areas throughout the world. Although there is no official quantification of groundwater level in North America, it is estimated by experts, that about 800 cubic kilometers worth of groundwater has already been depleted in the United States alone, in the 20th century. It is reported in one of the best-documented cases that 240 cubic kilometers amount of water has been removed in the United States in the 20th century; the case is of the Central United States, the 450k square kilometer High plain aquifer system. This is a reduction of about 6% of the predevelopment volume of water (McGuire et al., 2003). The depletion of groundwater, especially in some areas, has made it impossible to use the groundwater for agricultural purposes, as it is either very costly or almost impossible to get to the groundwater level (Dennehy et al., 2002). The depletion of groundwater not only removes groundwater but also has other effects as well. The residual groundwater from the groundwater pumping leaves behind the inferior quality of water, and also makes the groundwater prone and vulnerable to salinization, because of confining layers or adjacent aquifers that may be high in salinity or contamination. This is especially true in the context of coastal areas, when the freshwater is depleted, it is replaced by saline ocean water, as seawater starts to intrude (Konikow and Kendy, 2005).

In the context of Pakistan, the nation is very near to nationwide chronic water stress level. Rapid industrialization, urbanization, and population increase have already affected

the gap between supply and demand in the country. The country requires adaption of new sources of water and water conservation strategies and measures to use the finite and scarce freshwater most effectively as the number of drought years is increasing and the demand for freshwater is also increasing (Kahlowan and Majeed, 2003). At the bottom of the Indus River, due to the low of river water into the Arabian ocean, the seawater intrusion from the Arabian sea into the river and deltas has already begun and is causing damage to land, aquifers and increasing the salinity of water, which also affects the mangrove forests. The fish industry is also being affected in the Indus Delta, Karachi, and other cities and areas. The people of the affected areas are moving towards urban areas and this migration is pressurizing the already water-stressed cities of Pakistan like Karachi. As there is a huge gap between supply and demand and the population is increasing, this will most likely lead to frustration among the people which will lead to violence if the situation is not handled (Gizewski and Homer-Dixon, 1998; Qureshi, Shah, and Akhtar, 2003).

In Pakistan, irrigation of agriculture from groundwater has a long history. In the nation, the most difficult part of managing groundwater lies in the fact that there are numerous small-scale users of freshwater spread throughout the country. More than 80% of the groundwater pumping, takes place through these small-scale users, that is, private tube wells. There is no mark identification of these users, nor there is any registration process and there is no method of talking with these small-scale users to come to a consensus. In Punjab only, more than one-fourth of the total farmers are dependent on groundwater and Punjab counts for more than three fourth of the total land of agriculture in the nation. In addition to that, more than 60% of the farmers in Punjab use groundwater, in conjunction with canal water. This is a serious issue as the groundwater level is decreasing and a huge portion of the country's agriculture and the people will be facing water scarcity for agriculture and other purposes. The province of Punjab alone contributes to about 90% of the total agricultural production in the country meanwhile other provinces, Sindh and KPK, only produce 7%. Mainly because like in the province of Sindh, the groundwater is unfit to be used for agricultural purposes (Qureshi, Shah, and Akhtar, 2003).

Lastly, coming towards a part of our study area, Rawalpindi. Rawalpindi is the number 4th city in Pakistan in terms of area and the rate of urbanization in the city is

increasing due to the rapid increase in population. According to reports, the last three decades have seen an increase of 37.89% in urban areas. Most of this expansion of the city has occurred through deforestation and turning agricultural lands into residential and commercial lands. According to reports, the vegetation has decreased by about 45% in the urban city. Urbanization means more cementation and pavements which ultimately causes less seepage of rainwater into the groundwater and thus the recharge rate of groundwater decreases (Jat et al., 2009; McGrane, 2016). More of the rainwater runoffs and less of it can infiltrate into the groundwater aquifer. From the year 1990 to 2017, according to groundwater data, the groundwater level has shown a rapid decrease as the population and urbanization increased (Haq et al., 2021).

The city of Rawalpindi has experienced huge changes, in terms of Land Use and Land Cover, with the urban area increasing at an alarming rate of 50.22 ha per year. As mentioned above, there is also a huge decrease in the amount of vegetation. If this trend continues, then by the end of this century, the majority of the area of Rawalpindi will be urbanized. The rate of depletion of groundwater is estimated to be 1.38m per year. Meaning at this rate, the groundwater level will drop to 160m, by the end of this century, from the natural surface of the land (Haq et al., 2021).

1.3. Land Use and Land Cover (LULC)

The changes in physical and biological cover on land, including, forests, water bodies, soil, infrastructure, and agriculture etc. It is identified and marked by changes and activities performed by the community and how they change it or maintain it. Therefore, it is safe to say that people and their environment are linked via land use and land cover. So, in other words, we can say that Land Use and Land Cover means the Earth's land and soil cover change by anthropogenic activities. The drivers of these changes in land and soil are related to anthropogenic constructs like socioeconomic, demographic, as well as natural, like global and local climate and, big or minor, changes in the forest ecosystem (Chang et al., 2018).

The agricultural revolution, although started many centuries ago, never had effects that would alter and disturb the global system but now due to technological advancements,

humans have the capacity to bring about changes in the environment just from agriculture alone that if such activities are to be continued without bring sustainable changes and practices, there are going to be local, and global level unprecedented changed in ecosystem, ocean, and marine life etc. (Chang et al., 2018).

From 1850 to 1992, approximately, forests/woodlands and grasslands were cleared at amount of 6 million square kilometer and 4.7 million square kilometers, respectively (Ramankutty and Foley, 1999). From 2000 to 2010, the area under forest were decreased by 13 Mha per year (FRA, 2010). The croplands are being converted into residential and commercial areas, in some regions (Ramankutty and Foley, 1999). Meanwhile, simultaneously, the agricultural land has also increased in many regions, rapidly, from around 8 Mha to 47 Mha and finally to 2000 Mha since 1800, 1900 (Shiklomanov, 2000), and 2000 respectively (Siebert et al., 2005). Since 1900s, the rate of urbanization has evolved to more than 10 percent. Most of this rapid change has happened in Asia, Europe, and North America (Satterthwaite, 2007). With the advancement in technology and development of satellites, remote sensing has allowed the analysis or vast areas with precise practical and easily provided information; the software of remote sensing can also do analysis by sampling and assessment, find the cause of changes and the results of those changes (Chang et al., 2018).

The human survival depends upon environmental integrity and the food security, all of which can be measured by LULC analysis and that LULC is actually influenced due to human activities. Changes in LULC can affect the hydrothermal water cycles globally and locally. According to some research, for the last 10 decades, the emissions of Carbon Dioxide due to changes in LULC are equivalent to the burning of coal and other fossil fuels during the 1800s, which accounts to about 35% of the emission of Carbon Dioxide. And these emissions have direct influence on the global hydro-geo-chemical cycles of the world and also for the ecological balances. Thus, the addition of sustainable measures is essential for further advancement of to maintain the current level of modernization. The level of urbanization or forest cover, and other physical parameters, also determine the energy flow, balance, surface radiation, water cycle, water permeability etc. of the Earth. In addition to

spatial, temporal difference are also important as they play role in sustainable development control and others (Chang et al., 2018).

Thus, we can say that research in LULC has tremendous importance in the field of environmental sciences. Since the availability of satellite imagery and the software to manipulate it, researchers have done enormous amount of work to find results for policy makers. By two organizations: International Geosphere-Biosphere program (IGBP) and International Human Dimension Program on Global Environmental Change (IHDP), at the end of 20th century, was LULC proposed to have a better understanding of relation of human with their immediate environment. By this analysis and assessment, human activities and their influence on the ecosystem, ecology, and the changes in the environment has been observed; regarding both, the temporal changes, and the spatial changes. All of this analysis and assessment is to have an understanding for communities, policy makers and decision makers (Chang et al., 2018).

1.4. Significance of Land Use and Land Cover (LULC)

By using Land Use and Land Surface, we can calculate and analyze the effects of climate, economic and socio-political changes on people. When analyzed from a global point of view, these changes in LULC accounts for the changes in the system of the Earth as well. But it should be remembered that all changes are not bad. Some changes may contribute to food security safety and other for efficient utilization of resources and in overall wellbeing of humans. The followings points elaborate further as to why we use Land Use and Land Cover (Lambin et al., 2003).

1.4.1. Mapping urban areas:

Urban mapping is very important especially in our current era because mapping the urban area makes it easy for the policy makers and the decision makers to optimize the distribution of resources and also optimize the transport sector for sustainable development. This mapping has been now done for quite some time successfully using remote sensing (Schneider et al., 2009). Using remote sensing we can see how the urban areas have evolved over the past few decades. There are many methods for identifying and analyzing these urban changes like using (Cillis et al., 2021):

- Supervised Classification (Maximum Likelihood Classification)
- Vector Machine
- Decision Tree
- Wavelet Transform Developed
- Artificial Neural Network
- Linear Spectral Unmixing
- Support Vector Regression
- Vegetation Impervious Surface Soil Models (VIS)

These classification methods can be further divided into 3 subcategories:

- Pixel-based
- Subpixel-based
- Object-Oriented Methods

Among these, the pixel-based mapping is mostly used in urban mapping areas. But as the urban lands are developing more and more complex with variety of different structures and spatial extents, the second method, that is, the sub-pixel-based methods are becoming more popular. Especially in case of analysis in low resolution satellite imagery. For medium resolution imagery, Object-Oriented methods are becoming more famous as they allow to distinct between different textures of urban information (Cillis et al., 2021).

1.4.2. Urban expansion:

As we have talked about Urban Mapping, another aspect or urbanization is how rapidly it is extended in the rapidly rising population. This physical expansion of human made structures lies in Urban Expansion. This rapid urbanization is leading towards more and more complex landscapes which in return is causing changes in the structure and the functioning of the ecosystem. More urban area and more population means more consumption of resources and energy, which means more emissions of GHGs, which in return causes many problems like Climate Change and Urban Heat Islands. More urban land means more transportation and more industry which causes emission of other pollutants into the environment. This pollution is not only harmful for the environment but also for the human health as well. The urban areas also lead to changes in the

hydrogeological conditions as less water is able to leaches into the soil. Deforestation and transformation of cropland into urban area leads to loss in biodiversity as well as habitat fragmentation (Cillis et al., 2021).

Therefore, mapping the extension of urban area is crucial for sustainable development. And for that, satellite detection data methods rely on various change detection technologies, these detection technologies can be divided into three categories (Cillis et al., 2021):

- Visual Analysis & Digitized Changed Areas
- Classification Methods
- Post-Classification Methods.

1.4.3. Agriculture land:

In our rapidly changing population and urban areas, the assessment of food security is very important. And for this food security, guiding policies on sustainability are important, for that the use of agricultural land extension, changes and transformation is very crucial (Liu et al., 2005a; Yan et al., 2009). In the past, the changes in the agricultural land were determined by comparing the census data which was recorded over many years. But that method is not accurate and also don't give us information about the geographical spread. For that, remote sensing is excellent as it provides us both the spatial-temporal and geographical distribution (Amissah-Arthur et al., 2000; Doygun, 2009; Zhao et al., 2004; Zomeni et al., 2008). One of the most popular and straightforward method of detection in cropland changes is Post-Classification Method (Vorobyova and Smagulov, 2021).

1.4.4. Forest area:

In many parts of the world, the forests are being cleared like in tropical areas: Brazil, boreal Canada, and Siberia but at the same time, forests are also growing in many parts like the abandoned agricultural lands in the Eu and North America. All of these accounts for the changes in the local and global climate. For scientists to analyze the Carbon sinks and sources and how they are evolving and changing, and also for decision makers, the use of remote sensing is very important for monitoring these changes (Vorobyova and Smagulov, 2021).

1.5. Land Surface Temperature (LST)

Land Surface Temperature is a crucial parameter for the analysis of physical processes of energy on the surface level and water balances in any given place, either locally or globally; all of this is done by long-wave radiation and turbulent heat fluxes at the immediate air of the surface level and their interaction (Anderson et al., 2008; Brunsell and Gillies, 2003; Karnieli et al., 2010; Kustas and Anderson, 2009; Zhang et al., 2008). This information of the surface temperature and equilibrium state in Land Surface Temperature gives us the information about spatial and temporal changes (Kerr et al., 2000). Because of this it is widely used and studied in many aspects and phenomenon likes evapotranspiration, changing climate, the hydrogeochemical cycles, cropland and forest covers etc. (Arnfield, 2003; Bastiaanssen et al., 1998; Hansen et al., 2010; Kalma et al., 2008; Kogan, 2001; Su, 2002; Voogt and Oke, 2003; Weng, 2009; Weng et al., 2004), and is also recognized as one of the most important and of high priority parameter in IGBP (International Geosphere and Biosphere Program (Townshend et al., 1994; Li and Tang, 2014)).

A proper characterization of Land Surface Temperature is dependent on sampling in area variation and time variation as there are many factors that bring changes in the surface temperature that can be linked to the type of surface like forest, water body, urban area (Liu et al., 2006; Neteler, 2010) and the time variation, evolution, and distribution (Prata et al., 1995; Vauclin et al., 1982). Because of this time and spatial dependability, the measurement of surface temperature over a large area of land is impracticable using ground level monitoring devices. This is where remote sensing comes in to save the day. Using remote sensing and satellite imagery, which have evolved over time into much more high resolution, more spectrum of energy etc., the only possible way of measuring LST is through remote sensing. The thermal Infrared (TIR) sensor installed in satellites has a direct connect to Land Surface Temperature via RTE (Radiative Transfer Equation). The method of acquisition of LST using the TIR data dates back to 1970s and since then it has been used quite a lot and has gained reputation (McMillin, 1975; Li and Tang, 2014).

More than 10 percent accuracy of evapotranspiration and the Earth systems at very large scales can be attained and understood, given that the level of accuracy of LST is 1 K

or better (Kustas and Norman, 1996; Moran and Jackson, 1991; Wan and Dozier, 1996). But this level of accuracy is quite difficult as there are many factors that influence the values of Thermal Infrared like cloud cover, other atmospheric effects, and surface parameters (Li and Becker, 1993; Ottlé and Stoll, 1993; Prata et al., 1995). And for that reason, we have to calibrate the radiometric, cloud screening (removal of cloud cover), Emissivity and atmospheric correction (Li and Becker, 1993; Vidal, 1991; Li and Tang, 2014).

So far, we have defined what LST is, but we have yet to conclude its definition. But the thing is, there are no agreement about the definition of LST due to ambiguous physical meaning of temperature obtained from satellite, specifically in the case of different type and different thermal surfaces. The value of LST also depends upon:

- LSE (Land Surface Emissivity)
- R-Emissivity (Becker and Li, 1995)
- E-emissivity emissivity (Norman and Becker, 1995)
- Apparent Emissivity (Li et al., 1999)

The abovementioned emissivity is the same for same type of surface (homogeneous surfaces) but since in real life the surfaces are of different types (heterogeneous). Especially in low resolution satellites, the assumption of thermal equilibrium and homogeneity are transgressed. Thus, the differences between these definitions are crystal clear (Li and Tang, 2014).

1.6. Significance of Land Surface Temperature (LST)

The Land Surface Temperature moderates the temperature of the air in the urban area's lower layer and plays an important role in (Cillis et al., 2021):

- Energy exchange systems and radiation at surface
- The climate of the anthropogenic buildings, internally
- The thermal patterns of urban areas, their spatial extension, and their relation to the temperature of the surface
- Surface air temperature

- The well beings of humans and their comfort.

In simple terms, the Land Surface Temperature has been defined as the temperature of the ground's skin. The physics of our Earth surface processes are ruled by the LST and the combination of surface to atmosphere relationship and fluxes of energy between them.

- At micro level, within the urban areas, the urban heat islands are associated with the Land Surface Temperature.
- It also plays an important role at macro level of global thermal analysis, and also for heat balance studies in radiation budgeting.
- It controls the high temperatures by active radiation on the surface of the Earth, which is important for the energy stability of Earth.
- It also helps in finding the entrance of energy into the Earth surfaces and the fundamental heat fluxes.
- By studying LST, we also concluded that the changes in land cover and land use like development of anthropogenic infrastructure, cutting down forests etc., affects the climate of the globe.
- Thus, LST is an essential part of the Earth processes as many aspects depend upon them like thermohaline circulation, Climate, Urban climatology, anthropological and environmental interactions etc. (Weng, 2003; Ranjan et al., 2016; Cillis et al., 2021).

1.7. Geographical Information System (GIS) and Remote Sensing (RS)

GIS is a database that contains data of geographical locations and parameters, along with software tools and features to manipulate that geographical data. All of this is used to analyze, manipulate, and visualize those manipulations. The beauty of Remote Sensing, as indicated from its very own name, is that we can gather and acquire data of physical features of Earth without even having contact with it or moving to that location. Meaning anyone can see, analyze, manipulate, and visualize that information from any place on the Earth. The principal behind Remote Sensing is the electromagnetic radiations. These radiations are emitted from the source, mainly sun but sometimes satellite can emit these radiations themselves too. When these radiations strike Earth or atmosphere, they deflect

and reflect. Those radiations that reflect back into space are then captured by the satellites, which then analyze it and capture it in digital form. Over the years, the data from these satellites have become quite widespread, accurate, accessible in the recent years and are used in quite a lot of applications of different fields (Shannon, 2022).

1.7.1. ArcGIS software

Information concerning geography, or information related to a particular location or collection of locations on the surface of the Earth, as well as the zones of the atmosphere, is referred to as geographic information. Although in theory it might be interpreted to encompass information that is related to frames apart from the earth's surface, such as the human body (as in medical imaging) or a building, "spatial" is typically used synonymously with or even in preference to "geographic" in this context. Regardless of the reason for the transformation of geographical information in digital form, the word "GIS" is frequently used today. Thus, "GIS" refers to the process of creating a map using a computer. This involves analyzing geographic data on the same computer and applying sophisticated models of geographic processes to predict the future. While the earth images gathered by remote sensing satellites include geographical data, the systems that analyze the images are not to be referred to be GIS in such circumstances as long as they are restricted to this specific type of data. The term "GIS" is typically only used to describe systems that process previously cleaned and processed data or merge remote sensing data with other forms of data. Similar to this, an oceanographer or atmospheric scientist will typically identify "GIS" with the system utilized more for policy studies and transdisciplinary work, as opposed to other software environments for modelling and analysis within one's own profession (Liang and Wang, 2020).

GIS software, also referred to as geographic information systems, collects, analyses, and displays geospatial data to create two-dimensional or three-dimensional maps. GIS technology can recognize patterns and enhance performance in land-based operations since these tools serve as asset management platforms for the geographic information they collect. To advance its analytics capabilities, desktop GIS mapping software frequently interacts with a variety of drafting and design tools, such as BIM or CAD solutions. Additionally, these tools enable users to perform valuable analyses of

information like land usage and the location of geographical features like rivers or mountains, all from their desktop. In order to manage company operations, GIS software often focuses on collecting, analyzing, and displaying geographical data. GIS can be set up locally or in the cloud. Operational expenses may be reduced as a result of common implementations. To improve its analytics capabilities, GIS frequently interacts with CAD, BIM, and other drafting and design tools (Liang and Wang, 2020).

1.7.2. Remote sensing

The science and art of gathering data about an object, or more generally, the surface of the Earth, without coming into direct physical contact with it, is known as remote sensing. To do this, energy that is reflected or released is sensed, recorded, processed, analyzed, and put to use. Remote sensing uses sophisticated sensors to monitor the electromagnetic energy present in distant objects or geographic areas and then uses mathematical and statistical techniques to extract useful information from the data. It works with other geographic information sciences including cartography, surveying, GIS etc. (Liang and Wang, 2020).

Electromagnetic waves are typically categorized in remote sensing according to where on the electromagnetic spectrum they occur. The micrometer (m) is the most often used unit for determining wavelength along the spectrum. 1×10^6 meters make up a micrometer. There is no distinct boundary between one notional spectral region and the next, despite the fact that names (such "ultraviolet" and "microwave") are typically given to portions of the electromagnetic spectrum for convenience. Diverse ways of detecting each form of radiation have led to divisions in the spectrum, rather than intrinsic variations in the energy properties of different frequencies. It should be noted that the parts of the electromagnetic spectrum used in satellite imagery are distributed along a continuum with magnitude variations that range from several powers of 10 to many orders of magnitude. As a result, logarithmic graphs are frequently used to represent the spectral range (Liang and Wang, 2020).

1.8. Role of GIS and remote sensing in LULC and LST

Over the past 200 years, substantial changes in Earth's land cover have been a result of economic development and population growth, and all indications are that this trend will continue. A key element of contemporary strategies for regulating natural resources and tracking environmental changes is the change in LULC. Assessing and analyzing changes in land use and land cover has proven to be particularly significant when using remote sensing and geographic information systems. Recent advancements in digital image processing and remote sensing provide previously unheard-of chances to identify changes in land cover more precisely over expanding areas with decreasing prices and processing times. The current evaluations have examined a variety of detection techniques and come to a number of insightful results (Attri, Chaudary, and Sharma, 2015).

The processes through which items on the surface of the Earth change have their own temporal dynamics. Accurate change detection and object retrieval can both benefit from a better knowledge of these change processes. For change detection, multi-source data, particularly with distinct properties, are frequently required. The possible sensitive areas to shift as a result of the various driving forces can be identified using GIS-based analysis of the temporal data of LULC acquired from remote sensing of a region. The research agenda for change detection techniques in remote sensing is constantly expanding. Shift detection is a challenging process with no one best method that works in all circumstances. In order to comprehend the origin of this irreversible transformation, it is essential to evaluate the variations in LULC in terms of their spatial extent, intensity, and amplitude. A flexible framework for integrating data from multiple sources, processing steps, intelligent methods, and existing geographic information should be provided by the change detection methodology. The choice of an appropriate change detection method or algorithm for a particular research endeavor is crucial to obtaining reliable results because digital change detection is impacted by geographical, spectral, radiometric, and temporal restrictions. There is no one change detection method that works in every situation. Before using a suitable technique for the detector, it is important to take into consideration the characteristics of the study area, the sensor's spatial resolution, atmospheric effects, and sun angle in order to choose an appropriate way to detect change in an object or event on

the earth's surface. This paper briefly discusses three methods for detecting changes at the pixel, feature, and object levels. All of the binary change/no-change threshold methods have trouble separating actual altered areas from detected change areas. The methods that are advised are PCA and single band image differencing. Such issues can be avoided with classification-based change detection techniques, but they are more difficult to apply. When there is an enough amount of training data, post-classification comparison is an appropriate technique. GIS approaches can be useful when several sources of data are accessible. Higher quality results for change detection can be obtained using sophisticated approaches like ANN or a combination of change detection techniques. The object-oriented change detection approaches outperform pixel-based methods by reducing the effects of slight miss-registration between the two images, 'salt and pepper' noise, context relationships, and object shape information, as well as the effects of tree shadows and variations in sensor viewing geometry. By fusing approaches, soft computing approaches provide up new possibilities in this area. The applications' ability to go beyond the norm and try new things due to technical breakthroughs over the past few decades has fueled the development of remote sensing technologies (Blaschke et al, 2011). Development of efficient and effective change detection algorithms and frameworks that can search through enormous amounts of remote sensing data with various spatial, spectral, and temporal resolutions and enable change analysis are problems posed by the launch of new satellites (Vieira et al, 2012; Attari, Chaudary, and Sharma, 2015).

1.8.1. Mapping:

Measuring the location, scope, and dynamics of recent LULC is crucial for understanding land change research, and satellite remote sensing is frequently the only way to quickly inventory the land cover and track land cover change. long-term, systematic monitoring of land cover (Vorobyova and Smagulov, 2021).

1.8.2. Study of reactions and outcomes:

What are the effects of climate change and variability on LULC, and what possible feedbacks exist? How do land use activities adapt to and influence global environmental change, and what effects do changes in land use activities have on ecosystems? What

effects does LCLUC have on ecosystem sustainability and human societies? (Vorobyova and Smagulov, 2021).

1.8.3. Impact evaluation:

Both positive and negative effects of land use change might be biophysical and socioeconomic. Through the fragmentation of the landscape, variations in forest cover can have an impact on local water resources, biodiversity, and carbon sources and sinks. Changes in fire regimes can have an impact on water quality, aerosol emissions, trace gases, and ecosystem structure. Marginal lands that are overused become degraded and impoverished, which has an impact on human livelihood. Although fertilizer use in agriculture can increase agricultural productivity, it also has the potential to worsen water quality. By altering insect habitats or disease vectors, changes in land use can have an impact on human health. Land cover changes as a result of agricultural abandonment, such as an increase in woody vegetation. Agricultural fields and wetlands may be lost as a result of suburban and urban development (Vorobyova and Smagulov, 2021).

1.8.4. Urban development:

The local and regional climate can change as a result of land use changes. In order for scientists to calculate the change rates and their variations across time, they are crucial (Vorobyova and Smagulov, 2021).

1.9. Land-use Satellite (LANDSAT)

The mission of the spacecraft is to carry on the worldwide satellite imagery gathering program that the United States has been carrying out since 1972 with the aid of the Landsat series. The purpose of Landsat's Global Survey Mission is to repeatedly photograph the land and coastline regions of Earth in order to track changes to those regions over time (Vorobyova and Smagulov, 2021).

1.9.1. Landsat 8

Landsat 8 was launched in 2013 and Landsat 4-5 was launched in 1984. From 1900 to 2010, Landsat 4-5 were used, and from 2020–2022, Landsat 8 was used for Islamabad and Rawalpindi (EOS, 2022).

The LDCM satellite (Landsat Data Continuity Mission) was deployed from USS Vandenberg aboard an Atlas-V rocket on February 11, 2013. The mission of the spacecraft is to carry on the worldwide satellite imagery gathering program that the United States has been carrying out since 1972 with the aid of the Landsat series (EOS, 2022).

Operational Land Imager (OLI), a multichannel scanning radiometer, and TIRS, a two-channel IR radiometer, are among the remote sensing tools mounted on LDCM (Thermal Infrared Sensor). Advanced space photography technologies are used by the Ball Aerospace & Technologies-developed OLI instrument to produce images with a maximum resolution of 15 m at nine wavelengths between 0.43 and 2.300 m. They were created with the EO-1 experimental satellite (EOS, 2022).

The satellite's payload has a revolutionary design with fewer moving parts, extending its reliability and useful life by at least five years. The final photos have mapping accuracy of at least 12 meters. The Landsat series satellites can now make observations in two new wavelength ranges thanks to OLI, which is essential for examining cirrus clouds and the condition of lake and marine areas (EOS, 2022).

The images produced by the TIRS sensor have a spatial Landsat 8-pixel density of 100 m. In order to better understand the process of heat and humidity transfer for the agricultural industry, water management, etc., its primary goal is to measure surface temperature characteristics (EOS, 2022).

TIRS has the capability to undertake surveys in not just one, but two infrared wavelength Landsat 8 band combinations, in contrast to the hardware on board prior Landsat satellites. Compared to the transverse scanning instruments used on earlier Landsat satellites, both equipment shoots in scanning mode along the trajectory of the spacecraft, which lowers the level of radiometric distortion (EOS, 2022).

1.9.2. Landsat 4-5

Landsat 4 also featured a new scanning sensor with enhanced spectral and spatial resolution in addition to the MSS sensor. Seven spectral bands on these high-resolution scanners cover a 185 x 185 km² region. The Thematic Mapper (TM) scanner has the capacity to view the ground in higher detail and to monitor a wider segment of the

electromagnetic spectrum. The equipment contained seven spectral bands for gathering data from the electromagnetic spectrum's blue, green, red, near-infrared, mid-infrared (2 bands), and thermal infrared regions (EOS, 2022).

Two solar panels and both of Landsat 4's direct downlink transmitters were lost in 1983. Therefore, until the TDRS (Tracking and Data Relay Satellite) system was operational, data downlink was not feasible. In that situation, Landsat 4's Ku-band transmitter could send data to TDRS. Then, TDRS might transmit this data to its ground stations. Until it was decommissioned on June 1st, 2001, Landsat 4 remained in orbit for backup and data tracking. At that time, it was put into a disposal orbit to lessen the chance of colliding with other residing space objects (EOS, 2022).

Since its launch in 1984, Landsat 5 has collected more than 700,000 images, recording changes in the climate, agricultural methods, city growth and urbanization, ecosystem evolution, and the rising demand for natural resources (EOS, 2022).

Onboard Landsat 4 and Landsat 5, the Landsat Thematic Mapper (TM) sensor produced images with six spectral bands, each with a spatial resolution of 30 meters, and one thermal band (Band 6). The picture spans 170 kilometers north to south and 183 kilometers east to west (106 mi by 114 mi). TM could track locations where homes had been built or forestry had been removed, but it could not resolve specific dwellings or trees (EOS, 2022).

1.10. Problem statement

The rate of urbanization and urban expansion in the twin cities has increased dramatically in the past few decades, due to which LULC has been affected, mainly forest, vegetation, and barren land.

1.11. Objectives

This study has one main objectives:

1. Spatial-temporal analysis of LULC, to analyze how much changes have been observed in vegetation, forestry, settlement, barren lands, and water bodies, and in

Land Surface Temperature (LST), since 1990 to 2021, using LANDSAT 4-5, and LANDSAT 8 imagery, in geospatial tool (ArcGIS).

Chapter 2 - Literature review

2.1. Literature Review

A study conducted on Islamabad and its surrounding areas to determine the dynamics of land use and land cover changes using geo spatial analysis technique from 1992-2012 was accomplished by using supervised classification algorithm and application of post classification change detection technique in GIS. Analysis showed that urban areas, agricultural areas, and water increased during the study time period. While there was a substantial decrease in the forest and barren area. Generally, the change in water class was insignificant but for the major drinking water reservoir of the study area, there was a decline of 19.5% during 1992-2012. Moreover, environmental degradation resulted from the conversion of forest and barren land to urban due to population growth and economic development with a major negative urban development being the growth of the slums (Hassan et al., 2016).

A study conducted to analyze the influence of land use and land cover changes on urban heat island effect over Islamabad used remote sensing technique by taking 5 different images from 1995 to 2018. Spatiotemporal mapping of LULC and estimation of LST along with calculation of NDVI was done on the study area. The study area was classified into 4 classes namely, water, barren, vegetation and built-up. The results of this classification showed rapid growth in urbanization from 1995-2018 and the land cover patterns had changed significantly. While Islamabad's observed maximum air temperature in summer remained in the range of 20 to 45°C. While Islamabad's observed maximum air temperature in summer which remained in the range of 20 to 45°C. Regions with relatively higher LST were mostly concentrated in the north-east, due to the sparse vegetation along the south-east and south-west sides of the study zone. The development of small urban areas' roads is haphazard. The thermal disparity between the city and the environment outside the city showed a higher temperature contrast (Haider, 2021).

According to the study done on mountainous region of lower Himalayas for assessment of LULC and LST for the period of thirty years i.e., from 1987-2017, there was a considerable change in the LULC and LST. The urban area was increased by 4.43%,

agricultural area got reduced by 2.74% and waste land also decreased by 4.42%. land use changes effect land surface temperature which was observed when LST was highest for urban areas followed by barren, agriculture, and vegetation. the identification of patterns was done through support vector machine method using LANDSAT satellite images. The study also predicted the future LULC scenarios for the period from 2032-2047 using artificial neural network method. This method shows an increase in urban area that will increase the LST of 42-60% area to greater than 27 degrees Celsius in 2032-2047. Hence, all the results show that the study area is effected by climate change and global warming (Siddique et al., 2019).

For the investigation of LDVI in wabe sheble river basin, geospatial techniques and analytical hierarchy approach was used to model as well as access land degradation vulnerability. GMP, MODIS derived NDVI and LST were used for precipitation. Depth, texture, drainage, topography was also assessed along with precipitation for LDVI. According to the study, 17.06% of the area was very highly vulnerable to land degradation and 15.01% was highly vulnerable. NDVI followed by slope followed by temperature and precipitation are the most significant factors that determine the vegetation distribution and hence land degradation. Then through the use of AHP method and google earth images, land degradation vulnerability zone was modelled (Debele et al., 2021).

The review done on determining the dynamics of land-use and land cover change in the tropical regions, summarizes the estimates in land use changes that include cropland, intense agriculture, urbanization, and tropical deforestation. It establishes an interaction between climate driven climate driven land-cover and land use changes. moreover, the changes in ecosystem caused by the change in land use in turn act as drivers to land use changes. Use of complex adaptive systems and transitions can help understand the land use changes. The authors argues that a systematic analysis of local land use changes can help built general principles that that provide an explanation of new land-use changes (Lambin et al., 2003).

A study conducted in district of Lodhran, southern Punjab, Pakistan, for detection of land use and land cover changes for a time span of forty years develops a conclusion that vegetation cover gives a positive grounded connection with NDVI while open surfaces

and built-up areas give a negative grounded connection with NDVI for the mentioned time period. The study considered four major LULC types that is water bodies, built-up areas, vegetation, and soil. Patterns of LULC, NDVI, NDBI changes in Lodhran showed an increase in built-up area by 4.3 % as compared to 1977. LULC change with soil types, temperature, and NDVI, NDBI, and slope classes was common in the study area, and the conversions of bare soil into vegetation area and built-up area were major changes in the past 40 years in Lodhran district the conversion of barren land into agricultural areas or built-up areas over the period of 40 years has led to changes in land surface temperatures. The change in surface temperatures is prominent in the district with farmers facing the problem of rising temperatures, less irrigation water available and low precipitation. According to the study, the determination of LULC and LST changes help in division of policies and frameworks as well as strategies for the farmers in order to cope with the climate change (Hussain et al., 2020).

A study was done remote sensing-based quantification to derive the relationship between LULC and LST in the lower Himalayan region for the years from 1990-2017 as well as for the year 2032 and 2047. For the period of 1990-2017, the assessment of LULC and LST were done using Landsat data and support vector machine method while for the period of 2032 and 2047, a combined cellular automata and artificial neural network prediction model was used. The results showed that due to the inflow of population in the Himalayan region over the past decades has led to an increase in urbanization with an increase in built-up area by 5.57% and in bare soil by 4.22% while there was a decrease in vegetation cover by 9.88% during 1990-2017. The built-up area had the highest mean among all the other classes of LULC and LST. The prediction model anticipated that there will be a further increase in built-up area 12.485% in 2032 and by 14.65% by 2047. The area with temperatures above 30 degrees Celsius could be 44.01% and 58.02% in 2032 and 2047 respectively. As the land surface temperatures increased for all land cover classes, this clearly shows that urban warming and climate change are very much happening. The purpose of the study was to identify the challenge that urban planners have to deal with that is mitigation of urban heat islands. The solutions given by the study to the urban planners regarding this challenge is to work on both urban plantation and decentralization of urban areas (Ullah et al., 2019).

A case study of Guelma city of Algeria was done to build a relationship between LULC characteristics and LST using remote sensing and GIS. the city has been affected by massive urban growth which has increased LULC changes leading to climate change. the time frame was from 1986-2019. the LULC and LST were determined using Landsat images TM, ETM+ and OLI/TRS data, use of urban rural gradient, multi-buffer ring, statistics and techniques in urban landscape metrics were used for analysis. The results of the study showed that there was a remarkable increase in the urban areas of the city of Guelma with a decrease in green cover. With the change in LULC, there was a change in LST as well. according to the study, the years that witnessed a decline in vegetation cover that is 1986, 2000, 2005, 2010 and 2016 had the same temperatures which confirms the role of vegetation cover in decreasing the land surface temperatures. Moreover, over the years the gap between the temperatures of urban areas and forest areas has also widened as the urban area of the city saw an increase of 12% and a decline of agricultural and forest area by 15% and 3% respectively. Providing evidence of the increase in the gap between urban and forest areas, the study showed that their average temperatures of urban setting increased from 38.27 degrees Celsius in 1986 to 41.09 degree Celsius in 2019. Broad regions, a low landscape fragmentation degree and complex outlines have reduced forest LST values and increased urban LST values. In comparison to the LST of the sprawl form, the LST of the compact form is low. The results of the LST/NDVI and LST/NDBI relationship have shown a negative correlation and positive relationship, respectively. The study has shown the impact that urbanization and composition as well as form of landscape has on land surface temperatures. The knowledge obtained from the study will help policy makers of the Guelma city understand the complexities of LULC transition ,anticipate and schedule future changes in Guelma, achieve long-term stabilization of soil and water supplies and their effects on climate change (Imen et al., 2022).

A case study of Islamabad Pakistan related to LULC and its contribution to urban heat islands. The estimation of changes in LULC is done from 1993-2018. Anthropogenic influences on urban climate results in LULC changes due to urbanization and in turn effects LST the effects of the LULC on LST and relative LST for the city of Islamabad were observed using random forest classifier and standardized radiative transfer equation for LULC and LST respectively. The results showed an increase in built up area by 11.9% in

the time span of 26 years. The study reveals that due to the conversion of forests land, waterbodies and vegetation areas into in-built areas has caused a warming effect with a contribution of 1.52degree Celsius while the conversion of barren land and built-up area in to forests or water bodies have contributed to a cooling effect of -0.85degree Celsius on relative LST. Hence the positive(warming) contribution to UHIs is higher than negative (cooling)contribution. The study concluded that the LULC induced warming has increased over the region from 1993-2018 but there is still a need to do comprehensive investigation on the local and regional climate changes caused by LULC and LST changes. Lastly ,an intensive research in the future was also suggested specifically to investigate the proportion of green space and impervious surface and its impact on RLST for sustainable future cities (Khan et al., 2020).

Research done to analyze the LST in response to LULC changes in the region of Greater Cairo, Egypt using remote sending and GIS techniques. The region has experienced a surge in urbanization over the past few decades causing several environmental consequences. For the mitigation and proper management of such consequences. The process of assessment included generation of LULC maps which are derived from Landsat 5 TM for 1990 and 2003 and Landsat 8 OLI for 2016, using several classification techniques. A spectral radiance model and a web-based atmospheric correction model were used to successfully evaluate LST from thermal bands of Landsat data. Overall accuracy of Landsat derived land use data was 90.3%, 96.5% and 94.9% for years 1990, 2003 and 2016, respectively. The LULC change analysis revealed vegetation loss to urban land by an amount of 7.73% and from barren lands to urban uses by 8.70% within a 26-year timespan (1990 -2016). Results demonstrated the most distinct change was related to vegetation cover that drastically decreased by an amount of 32,097 ha (23.3%) from 1990 to 2016. In the same time period, significant reduction in barren land by 55,491 ha (8.70%) occurred. However, urban areas have significantly increased by 87,689 hectares (128.3%) because of the development of new industrial and commercial settlements, especially in the central and northern regions of the study area near water resources. over the entire study period from 1990 to 2016, the magnitude of LST increased by a rate of 2.06°C in areas that went from plant cover to urban and 2.60°C because of the conversion of barren lands from green areas. According to these findings, policies should

be put in place to lessen the negative effects of rising LST on sustainable development, population density should be controlled in ways other than just horizontal growth, green space should be improved with parks and gardens, and roof top areas should be planted with horticultural plants to lessen the impact of LST (Aboelnour and Engel, 2018).

Relative studies done in China regarding the land use and land cover change for the mid-90s to establish national operative dynamic information serving systems on natural resources and environment. For the study of Land use/land cover changes, the research used 520 scenes of remotely sensed images of Landsat thematic mappers which were interpreted in to LULC categories at a scale of 1:100,000 under digital environment. The data was georeferenced and Orth-rectified as well...the vector map of the resolution mentioned was then converted to a 1km raster database that calculated the area percentage for each kind of land use category. A series of studies have been implemented based on LULC a database. moreover, based on this database a spatial and temporal database has been established to support the research related to earth sciences. The knowledge innovative projects from these national information and database will also integrate the accumulated data covering environmental, regional, social and economic fields (Jiyuan et al., 2002).

A review done for metrology and climatology on remote sensing of land surface temperatures reviewed the satellite, sensors, and studies relevant to land surface temperature measurements with the focus laid on the use of thermal infrared part of EMR spectrum. The reason being to ensure useful use of land surface temperature which can be beneficial for number of uses including the measurements of urban heat islands. According to the authors, there is a huge research gap in quantification of the relationship between measured air temperatures and remotely sensed LST data. This information is important for policy makers and urban planners to make decisions that must be communicate outside the scientific community. The authors of the research review say that there is an increasing need for data analysis which in turn puts necessity of using remote sensing data along with other data sets. therefore, this results in an integral role for remote sensing techniques in meteorology and climatology (Tomlinson et al., 2011).

Table 2.1: Literature review table

Sr.No	Study	Region	Method	Study Topic
1	(Hassan et al. 2016)	Islamabad, Pakistan	supervised classification algorithm and post - classification change detection technique	The dynamics of land use and land cover changes using geo spatial analysis technique in Islamabad and surrounding areas
2	(Haider 2021)	Islamabad, Pakistan	Satellite based remote sensing and object-oriented classification	Analysis of the influence of land use and land cover changes on urban heat island effect over Islamabad used remote sensing technique
3	Siddique ullah a , Khalid ahmad a , Raja umer sajjad a , Arshad mehmoood abbasi a , Abdul 2019)	Lower Himalayan region research study	Remote sensing and artificial neural network technology.	Simulating current and future land cover changes and their impacts on land surface temperature in a lower Himalayan region authors
4	(Debele et al., 2021)	Wabe sheble river basin	Geospatial techniques and analytical hierarchy approach	Modelling and accessing land degradation vulnerability using remote sensing
5	(Lambin et al., 2003)	Tropical regions	geospatial techniques	Dynamics of land use and land cover changes
6	(Hussain et al., 2020)	Lodhran district, Pakistan	Supervised classification and LST equations	Detection of land use and land cover changes using GIS tools
7	(Rahman et al., 2022)	Northern KPK, Pakistan	Maximum probability classification and radioactive transfer equation method	Modelling of land use/cover and lst variations by using gis and remote sensing

8	(Ullah et al., 2019)	Lower Himalayan region	Support vector machine method and artificial neural network prediction model	Remote sensing-based quantification of the relationships between LULC and surface temperatures
9	(Imen et al., 2022)	Guelma, Algeria	urban rural gradient and multi-buffer ring	Relationship between LULC characteristic and LST using remote sensing and GIS
10	(Khan et al., 2020)	Islamabad, Pakistan	Random forest classifier and standardized radiative transfer equation	Land-use / land-cover changes and its contribution to urban heat island
11	(Aboelnour & engel, 2018)	Greater Cairo region, Egypt	Classification techniques and spectral radiance model	Application of remote sensing techniques and GIS to analyze land surface temperature in response to land use/land cover change
12	(Jiyuan et al., 2002)	China	Digital software environment	The land use and land cover change database and its relative studies
13	(Tomlinson et al., 2011)	Global	Use of thermal infrared part of EMR spectrum	Remote sensing land surface temperature for meteorology and climatology

2.2. Rationale of the study

The focus of our study was to determine the rate of urbanization and causes of its expansion. We also wanted to see the rate of deforestation and how urbanization contributed to the Land Surface Temperature of the study area. Previously, some similar studies have been conducted and their findings are as follow.

Ghafoor et al. (2022) conducted a study on impacts of LULC on Soan Valley Ecosystem. The restricted anthropogenic activity in HM forest caused an increase of about 32% in vegetation density thus from 2007 to 2019 carbon was accumulated in biomass. This is due to the implementation of Punjab Forest Act 2010 and considerable decline in livestock grazing from past 10 years.

Ullah et al. (2019) conducted a study on LULC and LST on Lower Himalayan region. Their study included settlement, vegetation cover, barren land, and water bodies for LULC, which was conducted over the year of 1990 to 2017. For the period of 1990-2017, the assessment of LULC and LST were done using Landsat data and support vector machine method while for the period of 2032 and 2047, a combined cellular automata and artificial neural network prediction model was used. The results showed that due to the inflow of population in the Himalayan region over the past decades has led to an increase in urbanization with an increase in built-up area by 5.57% and in bare soil by 4.22% while there was a decrease in vegetation cover by 9.88% during 1990-2017. The built-up area had the highest mean among all the other classes of LULC and LST. The prediction model anticipated that there will be a further increase in built-up area 12.485% in 2032 and by 14.65% by 2047. The area with temperatures above 30 degrees Celsius could be 44.01% and 58.02% in 2032 and 2047 respectively. As the land surface temperatures increased for all land cover classes, this clearly shows that urban warming and climate change are very much happening. The purpose of the study was to identify the challenge that urban planners must deal with that is mitigation of urban heat islands. The solutions given by the study to the urban planners regarding this challenge is to work on both urban plantation and decentralization of urban areas.

Khan et al. (2020) conducted a study on LULC and urban heat islands in the city of Islamabad, Pakistan. The estimation of changes in LULC is done from 1993-2018. Anthropogenic influences on urban climate results in LULC changes due to urbanization and in turn effects LST the effects of the LULC on LST and relative LST for the city of Islamabad were observed using random forest classifier and standardized radiative transfer equation for LULC and LST respectively. The results showed an increase in built up area by 11.9% in the time span of 26 years. The study reveals that due to the conversion of forests land, waterbodies and vegetation areas into in-built areas has caused a warming effect with a contribution of 1.52 degree Celsius while the conversion of barren land and built-up area into forests or water bodies have contributed to a cooling effect of -0.85 degree Celsius on relative LST. Hence the positive (warming) contribution to UHIs is higher than negative (cooling) contribution. The study concluded that the LULC induced warming has increased over the region from 1993-2018 but there is still a need to do

comprehensive investigation on the local and regional climate changes caused by LULC and LST changes. Lastly, intensive research in the future was also suggested specifically to investigate the proportion of green space and impervious surface and its impact on RLST for sustainable future cities.

Rahman et al. (2022) conducted a study on Northern Pakhtunkhwa mountainous region of Pakistan for modelling of LULC and LST variations examined 30 years changes in LULC and LST i.e., from 1987-2017. significant changes were found in LULC especially the built-up area and bare soil area which in turn has affected LST. The examination of these changes was done by developing LULC maps based on maximum probability classification, LST from Landsat thermal bands and radioactive transfer equation method for the set timeframe. For future prediction weighted evidence, cellular automata and regression prediction models were used. The results of LULC classification showed an increase in built-up area and bare soil classes by 13 km² and 89 km² respectively while there was a decrease in vegetation classes by 144 km² during 1987-2017. For the same time span, for LST, the temperature range increased by 140 km² for the next 30 years i.e., till 2047, the findings show similar trend for each class. According to the authors, the study has provided a significant insight for monitoring of urban development, for climatologists and land use planners of urban heat island formations. it is also an alarm for the developmental projects in the study area which include both CPEC project and the Tarbella dam in such environmentally sensitive region.

Chapter 3 - Materials and methods

3.1. Study area

The capital of the Islamic Republic of Pakistan, Islamabad, is situated in the Potohar plateau between 33°28'00" N in latitude and 72°48'00" E in longitude. Its 906 km² territory includes mountains and uneven plains that peak more than 1,175 m elevated above the average sea level (Sheikh et al., 2020). The inner boundary in the figure 1 shows the city of Islamabad, the outer shows the boundary of city of Rawalpindi (Sheikh and Pasha, 2007).

In the Potwar Plateau, close to Islamabad, sits the city of Rawalpindi. In terms of latitude, Rawalpindi is located between 33° 28' and 33° 48' north and 72° 48' and 73° 22' east in terms of longitude. The city is bordered on the north and east by the Islamabad region, and on the west by the highway and the cities of Taxila. The region of Rawalpindi covers 250 square kilometers and extends all the way to Islamabad, the country's capital (Adeel, 2010).

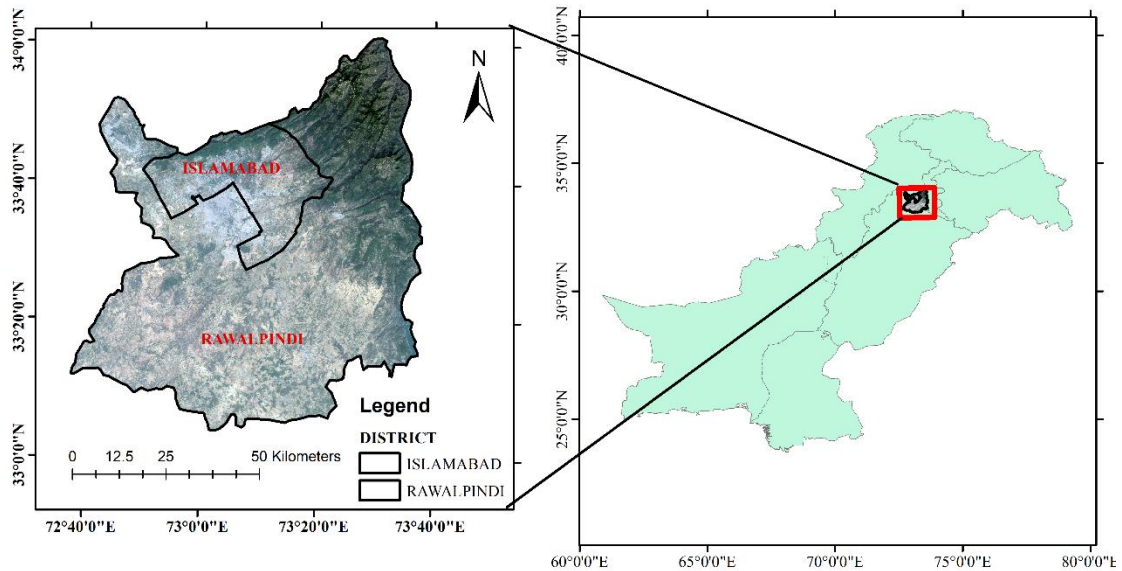


Figure 3.1: Study Area Map

3.2. Materials and methods

The images for the supervised classification of Water, Barren, Vegetation, Forest and Settlement were taken from United States Geological Survey, of LANDSAT 4-5 satellite for the year 1990 to 2010, and LANDSAT 8 for the year 2021. The same image's bands were used (namely: NIR, R, and TIR) for the calculation of LST using different equations in ArcGIS.

3.2.1. Satellite imagery data acquisition

The following table shows which imagery was taken for each decade with month included, the type of satellite, its sensor, its resolution, its row & path with source as well.

Table 3.2: Satellite imagery data acquisition

S. No	Satellite	Time period	Sensors	Resolution	Row/Path	Source
1	LANDSAT 4-5	October 1990	MSS	30m x 30m	36/150, 37/150	https://earthexplorer.usgs.gov/
2	LANDSAT 4-5	October 2000	MSS	30m x 30m	36/150, 37/150	https://earthexplorer.usgs.gov/
3	LANDSAT 4-5	October 2010	MSS	30m x 30m	36/150, 37/150	https://earthexplorer.usgs.gov/
4	LANDSAT 8	October 2021	OLI, TIRS	30m x 30m	36/150, 37/150	https://earthexplorer.usgs.gov/

3.2.2. Image Processing of Land use and Land Cover (LULC)

For the calculation and analysis of the Land Use and Land Cover, the sequences, and steps we took can be summarize in simple way as: we first took the whole map of Pakistan by district, then removed the study area of interest. After that we downloaded and imported the satellite images that covered the entire study area. The images came out to be in two rows of same path, so, we had to combine the two images together, then remove the areas of images that were not the part of our study area. After that we started the assessment of LULC by using maximum likelihood classification. For that, for each class:

Urbanization, Forest, Vegetation, Barren and Water, we took 500 training samples for each class.

3.2.2.1. Clipping

Clipping geoprocessing tool is a method of separating a dataset by utilizing one or more than one features in another dataset. This is also particularly helpful for creating new datasets, also called the study area or area of interest, AOI, which contains the geographical region on which further analysis is to be done (ESRI, 2022).

Clipping geoprocessing tool was used to separate the study area or area of interest, that is, Rawalpindi and Islamabad, from all the districts of Pakistan.

3.2.2.2. Imagery imports

After separating the area of interest, which was a blank solid color polygon that contained the boundary of the area of interest and also the coordinates. To input the actual geographical features and the actual area imagery, we used satellite imagery. The satellite images were taken from USGS (United States Geographical Survey). The Path and Rows of the study area came out to be 150036 and 150037 (150: path and 36, 37: Row). These two images covered more than all the study area and were overlapping.

3.2.2.3. Composite

Before explaining the composite, it is worth mentioning that composite was only done for Land Use and Land Cover (LULC) and not for Land Surface Temperature (LST).

- Composite tool is used when a dataset which contain subsets of the ‘whole’ original raster dataset bands is used to combine all together to create a new raster dataset which contain specific band combinations and order.
- The order of the bands is also important which determine the output of the new raster dataset. But this tool can only be used on a square raster cell.
- There are many different output or export file exertions that this new raster dataset can be exported as, like, TIFF, PNG, JPEG, etc. The first raster band’s cell size in the list is used to make the new output raster dataset.

- The output of the composite contains all the coordinates references and the extent of the original raster dataset imagery (ESRI, 2022).

3.2.2.4. Mosaicking

Mosaicking is used to combine or merge two or more satellite images into one image. The overlap sections that were previously overlaid over each other become one accurate combined image. In ArcGIS, it is possible to create a single raster image from many raster images. It is done by searching for **“Mosaic to new Raster (Data Management) tool”**, in the search option (ESRI, 2022).

3.2.2.5. Masking

After combining the images, the covered area more than the actual study area, the need for removing the extra image was needed so only the study area was covered. This was done by masking. Masking is basically hiding the unwanted and unnecessary parts of the image from the study area or area of interest. It is done by searching for **“Extract by mask (Spatial Analyst) tool”** (ESRI, 2022).

3.2.2.6. Maximum Likelihood Classification

In Supervised image classification, we need to train the computer to analyze the pixels or polygons that we assign as classes and then based on that the computer then analyze the extension or the total area that each class covers in the whole map. These training samples can be managed from Training Sample Manager panel. About 500 training samples were taken for each class: Urbanization, Water, Barren, Forest, and Vegetation. After that, a signature file was created from these 500 points of the 5 classes. Using this signature file, from the classification panel, maximum likelihood classification was undergone which then gave us the amount of total area that was covered by each class (ESRI, 2022).

3.2.3. Image classification

The following tables shows the band combinations of each LANDSAT satellite. These bands were used to identify and locate different classes: Urban, Water, Forest, Barren and Vegetation.

Table 3.3: Bands combination of LANDSAT 4-5, and LANDSAT 8

Type of Color	LANDSAT 4-5	LANDSAT 8
Infra-Red	4, 3, 2	5, 4, 3
Natural color	2, 3, 1	4, 3, 2
False color (Vegetation analysis)	5, 4, 3	6, 5, 4
False color (Urban)	7, 5, 3	7, 6, 4
False color	7, 4, 2	7, 5, 3

The following table shows the classes which were taken for identification and everything that is included in those classes.

Table 3.4: The five Classifications

Class	Includes:
Urbanization	<p>All man-made structure such as</p> <ul style="list-style-type: none"> • Highways and roads • Bridges • Airports • Railway stations • Buildings • Dams structure • Housing societies. • Industries
Forest Area	<p>Natural forest and features need to be included so that they are considered forest are high animal and vegetal biodiversity, evergreen trees, dark and sparse undergrowth interspersed with clearings, scanty litter (organic matter settling on the ground), presence of "strangler" creepers.</p> <ul style="list-style-type: none"> • Areas that come inside the forested area in our study area are:

	<ul style="list-style-type: none"> • Margalla Hills • Northern parts of Islamabad and Rawalpindi • Small patches in F9, and Ayub Park • Miyawaki forests • Wah cantonment and surrounding areas
Vegetation Cover	<ul style="list-style-type: none"> • All agriculture • Parks • Man-made vegetation • Green belt • Gardens • Small Patches of trees • Grasslands
Water Bodies	<ul style="list-style-type: none"> • River • Ponds • Lakes • Lagoons
Barren land	<ul style="list-style-type: none"> • Infertile arid land • Recently harvested land which was clear for new crops • Land cleared for future construction • Deforested land

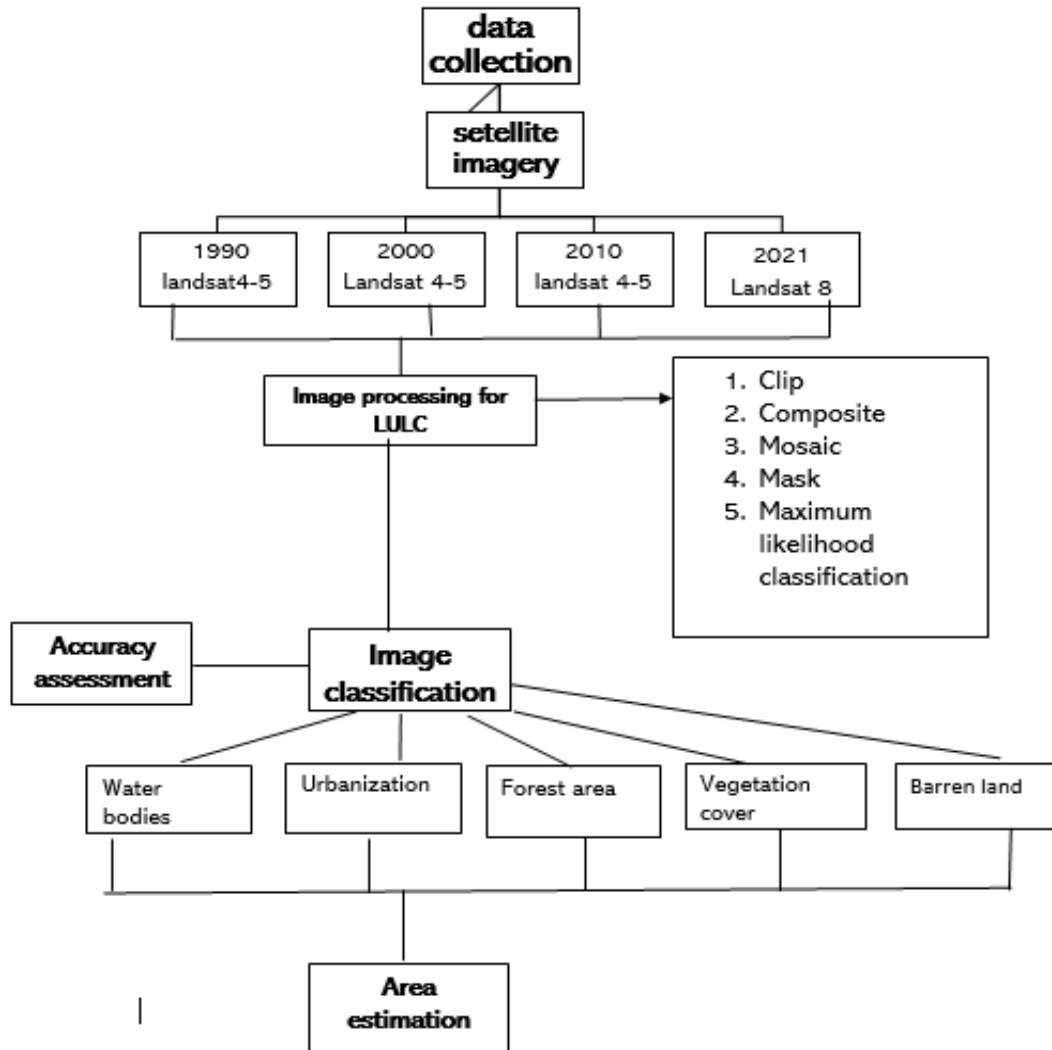


Figure 3.2: Methodology of LULC

3.3. Image Processing for Land Surface Temperature (LST)

For the derivation of LST from the geometrically corrected Landsat images, there is a six-step process that converts the thermal data acquired by Landsat sensors and stored in digital numbers in to LST.

The thermal infrared bands, near infrared bands and red bands of different Landsat image types were taken. for Landsat 4 & 5 TM band 6, band 3 and band 4 were thermal, near infrared and red bands respectively (for years 1992, 2000 and 2010). For Landsat 8, band 10, band 4 and band 5 were the thermal, near infrared and red bands respectively (for year 2021).

For each year, two sets of thermal, near infrared and red bands were selected from the tiles representing the study area and added to arc map where each set of the three bands from both the tiles are first mosaiced, then masked and then by using raster calculator of Arc map the 6 step mathematical process is done. The tiles were not processed to composite because the information in the meta data file of both tiles was same for all the years.

The steps below are employed to retrieve LST from thermal images and NDVI images. Following are the steps for LST. All the numeric values are driven from metadata text file.

3.3.1. Top Of the Atmosphere calculation (TOA)

TOA is a unitless measurement which provides the ratio of radiation reflected to the incident solar radiation on a given surface. The thermal emissions from the earth are captured in the form of raw digital numbers which is converted to luminance radiation or top of the atmosphere radiances (TOA) by the following equation:

$$L_{\lambda} = ML \times Q_{cal} + AL$$

Where:

L_{λ} is the luminance radiation or top of the atmosphere

M_L is the being the Band-specific multiplicative rescaling factor from Landsat metadata.

Radiance_Multi_Band_X, where x is the band number

X = 6 for Landsat 4&5

x = 10 for Landsat 8

Q_{CAL} = Quantized and calibrated standard product pixel values (DN)

AL = is the specific additive rescaling factor band from the metadata

3.3.2. Brightness Temperature calculation (BT)

The brightness temperature, which is described in terms of the temperature of an equivalent black body, is a measurement of the radiance of the microwave radiation moving upward from the top of the atmosphere to the satellite. Brightness temperature is

calculated using radiance images which were obtained from thermal bands (Chander, Markham, and Helder 2009). The formula for BT is as follows:

$$BT = \frac{K2}{\ln\left(\frac{K1}{L\lambda + 1}\right)} - 273.55$$

BT is brightness temperature

K2= is the prelaunch calibration constant 2 in Kelvin.

K1: is the prelaunch calibration of constant 1 in unit of W/ (m²sr·°m)

L_λ: luminance temperature /top of the atmosphere

3.3.3. Normalized Differential Vegetation Index (NDVI) calculation

NDVI stands for Normalized differential vegetation index. The quantity and vigor of the surface plants are gauged by the NDVI index. Because vegetation reflects light strongly in the near infrared region of the spectrum, the NDVI has evolved into a straightforward graphic indicator for gauging target vegetation coverage. As it can account for shifting lighting conditions, surface slope, and viewing angle so it is particularly helpful for monitoring vegetation at a continental to global scale.

The formula for NDVI is as follows:

$$NDVI = \frac{NIR - Red}{NIR + Red}$$

where Red and NIR are the spectral reflectance of vegetation,

NIR: is the near infrared band,

Red: is the red band

3.3.4. Proportion of Vegetation calculation (PV)

POV is defined as the ratio of the vertical projection area of vegetation (containing leaves, stalks, and branches) on the ground to the total vegetation area. POV can be derived from the NDVI image based on the following equation:

$$POV = \left(\frac{NDVI - NDVI_{min}}{(NDVI_{max} - NDVI_{min})} \right)^2$$

Where:

NDVI_{max} is the highest value of NDVI

NDVI_{min} is the lowest value of NDVI

3.3.5. Emissivity calculation (ϵ)

Emissivity is defined as the ratio of the energy radiated from a material's surface to that radiated from a perfect emitter, known as a blackbody, at the same temperature and wavelength and under the same viewing conditions. The emissivity is calculated with the following equation:

$$\epsilon = 0.004 \times P_V + 0.986$$

Where:

P_V is proportion of vegetation

3.3.6. LST calculation

The Land Surface Temperature (LST) is the radiative skin temperature of the land surface, as measured in the direction of the remote sensor. Outputs derived from above equations were then used as inputs to estimate the LST using the equation below:

$$LST = \frac{BT}{\left(1 + \frac{\lambda BT}{p} \ln(\epsilon)\right)}$$

Where:

λ : is the central wavelength (in μm) of the Landsat thermal band,

$$p = 1.4388 \times 10^{-2} \text{ mK}.$$

ϵ = emissivity

$$\lambda=0.00115$$

BT=brightness temperature

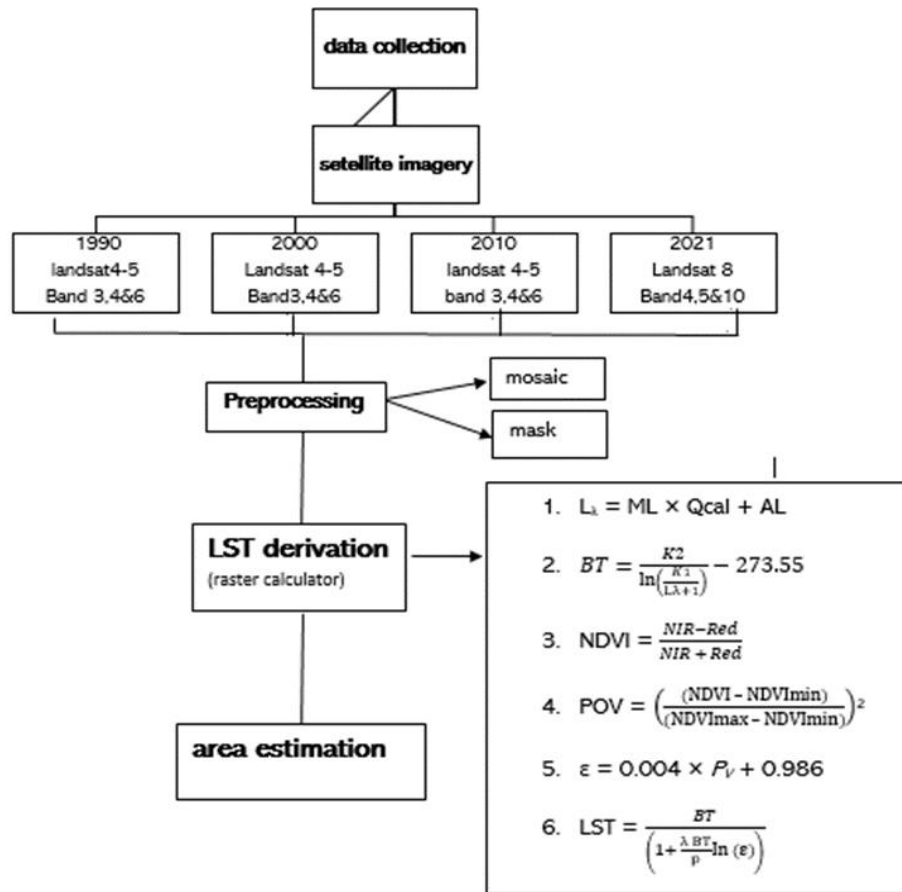


Figure 3.3: Methodology of LST

3.4. Accuracy assessment

Accuracy assessment is an important step in analyzing the land classification. Following steps are taken to perform an accuracy assessment for a classified image. We extracted pixel values from reference points, create an error matrix, calculate the overall percent accuracy. The user's accuracy and producer's accuracy. Assessing the accuracy is a good check point to determine whether there is a need to resample the classification or ready to move forth with the analysis.

3.4.1. Marking of reference points on Google Earth pro

50 points were taken in Google Earth Pro on the same study area as the ArcGIS. This was done to calculate the accuracy of the LULC calculated in ArcGIS. For an example, points of year 2021 are shown in the figure below.

3.4.2. Sequencing of Earth pro points and ArcGIS points

The points on Earth Pro (Reference point) should be placed in a way that they match the locations with the points on ArcGIS map. The sequence of the point should be same as the ArcGIS to reduce any sort of error in calculations and get correct accuracy. To extract the earth pro points and their pixel values into ArcGIS we need to convert the KML file where the earth pro points are saved into layer file in the ArcGIS, go to search write KML to Layer from there add the information required.

3.4.3. Extract value to points

We want to obtain the pixel value for each point so that we can compare them to our categorized image now that we have loaded all of the identical points. We first go to Spatial Analyst Tools, pick Extraction, Extract Values to Points, add the data, and then select each reference point's pixel values. Once the processing is finished, you should add the new file to your map. The classified values are in the field RASTERVALU when you right-click on the new Values.shp file in the Table of Contents and choose to open the attribute table.

After that, select Add Field under Table Options. Give this field the name Classified. Select Short Add Feld Name Cashed Integer as the type, then click OK. Right-click the newly added Classified column once it has appeared and select Field Calculator. The message "You are about to do a calculation outside of an edit session" can appear. Select Yes. Double-click OK in the Field Calculator's Fields section. Click OK after selecting Cancel and RASTERVALU. As a result, the data will be moved from the RASTERVALU column to the Classified column. To rename Values to Reference, follow the same procedure. Rename the Reference field by selecting Add Field. Select Short Integer as the type. Click the new Reference column with the right mouse button, pick the Field Calculator, click Values, and then click OK. Remove the Value and RASTERVALU columns. Right-click the RASTERVALU column and choose Delete Field to accomplish this. Click Yes when you receive the Confirm Delete Field warning. Sort the table using the categories of land cover that we listed in our categorized image for clarity. Select Sort Ascending from the context menu by selecting the Reference column.

3.4.4. Frequency table

After having the values of the reference points through the above-mentioned steps, the frequency values for the classified image and reference points are isolated.

Navigate to frequency tool using the arc toolbox or by using the search option of ArcGIS. Fill in the fields of frequency window and save the file in .dbf format. When the process gets complete, the frequency table appears under the values file in the table of content. The frequency table shows how many pixels were correctly predicted in the Landsat image for each reference point marked. Although the frequency table provides information but it's still hard to read. This information can be put in an easier form through the next step.

3.4.5. Error matrix

A pivot table must be created to sort and display the frequencies. Navigate the pivot table tool from arc toolbox, fill the fields of the pivot table window and save it as an error matrix in .dbf format. When the process is done, open the attribute table of the newly created error matrix table in the table of content and ensure that all the land cover classes are present along with same number of reference points in the table. If all the classes are present the process done is correct.

The .dbf format of error matrix is converted in to .xls format by navigating to the table to excel tool and saving it in accuracy assessment folder for further calculation.

3.4.6. Accuracy assessment final table

The accuracy image is the often reported as a percentage correct. There are different types of accuracy that must be calculated which includes overall accuracy, user's accuracy, and producer's accuracy.

The error matrix in the .xls format saved in the previous step is opened which shows reference data in columns and classified data in rows.

The classes are labelled as numbers that have to be renamed under the classified column. Add a column of total reference points and total classified points where the sum of the reference points and classified points are deduced respectively.

Next is the calculation of total correct reference points in order to calculate the error for which the sum of the pixel values is correctly matched and divided by the total reference points. After this the percent accuracy is calculated by dividing the total corrected reference points by total reference points. This will give the percentage accuracy for that particular year.

After this, the next two accuracies to be found are user accuracy and producers' accuracy. The producer's accuracy column shows false negatives, or errors of commission. The data to compute this error rate is read in the columns of the table. The Total column shows the number of points that were identified as a given class, according to the classified map. The producer's accuracy is found by dividing the diagonal number by the column total and multiplying by 100.

User's accuracy is also referred to as errors of commission, or type 1 errors. The data to compute this error rate is read from the rows of the table. The Total row shows the number of points that should have been identified as a given class, according to the reference data. The user's accuracy is found by dividing the diagonal number by the row total and multiplying by 100.

Chapter 4 - Result and Discussion

4.1. Study area's parameters description

4.1.1. Geology and general topography

The geography in the Islamabad-Rawalpindi metropolitan region is made up of plains and mountains with a combined elevation of more than 1,175 m. Three main geomorphologic zones all have an east-northeast pattern. The upper and outer Himalayas, comprised of the Hazara as well as Kala Chitta Ranges, are home to the mountainous Margalla Hills, which is where the northern portion of the metropolitan region is located. The Jurassic through Eocene limestone and shale ridges that make up the Margalla Hills, which rise to a height of 1,600 m close to Islamabad, are intricately thrust, folded, and typically overturned (Sheikh et al., 2007).

Located south of the Margalla Hills, the Rawalpindi Group's folded sandstones and shales form the majority of the piedmont bench's subsurface (Miocene). Despite having broad plains of wind-blown silt and typically low relief, the piedmont region also contains numerous ridges and valleys that have also been submerged by alluvial deposits from the hills. Sandstone ridges that have been buried are typically covered by interbedded layers of sandy silt and limestone gravel that are more than 200 meters thick in some places. These deposits have been cut into pieces and then buried beneath an eolian loess and reworked silt layer that is more than 40 meters thick in some places. Because they make up the majority of building structures and because gravel serves as the main ground-water aquifer, the gravel and loess are particularly significant to environmental geology. Shallow badland valleys are extensively cut into thick, readily eroded loess plains west of Rawalpindi. East of Rawalpindi, significant hills are formed by the folded ridges of Rawalpindi Group rocks rising above the alluvial plain. The piedmont bench area is where the majority of urban development is focused. Rawalpindi is located in the southern portion of this area, close to the Soan River, whereas Islamabad is located in the northern section of the piedmont bench area, which is less deeply divided (Sheikh et al., 2007).

The Soan River valley stretches typically along the axial direction of the Soan syncline at an altitude of around 425 m in the southernmost part of the region. The Soan is

cut more than 40 m below the level of the vast plains north and south of the river, which are covered with silt. The Soan canal and flood plain span 1.5 kilometers over the valley floor southeast of Rawalpindi, upstream from the Grand Trunk Road bridge. The valley bottom is even narrower in other places. The southern region is underlain by fluvial sandstone, mudstone, and conglomerate beds from the Neogene to Pleistocene Siwalik Group, which also appear along the numerous steep-sided stream valleys that cut the landscape. The beds drop more gradually on the south limb of the syncline than they do on its north limb, which is north of the Soan River. The northern edge of the Potwar Plateau, which stretches 150 km southwest, is comprised of the piedmont bench and the Soan valley (Sheikh et al., 2007).

4.1.2. Population trend

The national capital and the core of all governmental operations is Islamabad; the industrial, commercial, and military presence is concentrated in Rawalpindi, a larger and older metropolis. Along the historic trade route that connected Persia, Europe, and India via the Khyber Pass is Rawalpindi. Alexander the Great, Genghis Khan, the conquerors of the Moghul Empire, and other notable historical personalities have all travelled through the region, which has long been a crossroads of cultures and an incursion route. When it became a crucial staging area for the British Afghan wars in the late 1800s, Rawalpindi, which had been inhabited before 1765, gained prominence. The Pakistan Armed Forces' administrative center and a significant military cantonment are still located there. To serve as the capital of Pakistan's newly independent nation, Islamabad was built in a picturesque location at the foot of mountains north of Rawalpindi. Following thorough surveys and planning, construction started in the early 1960s. Since then, Islamabad and Rawalpindi have had tremendous population expansion, with a combined population estimated is estimated at 1.3 million. This has led to an increase in the demand for natural resources and negative consequences on the environment (Sheikh et al., 2007).

4.1.3. Hydrology

The primary rivers that drain the region are the Soan and Kurang Rivers. The Ling River, which empties into the Soan from the northwest; Gumreh Kas, which empties into the Kurang from the region between the Kurang and the Soan; and Lei Nala, which empties

into the Soan from the mountain front and populated areas; are their principal tributaries. For the purpose of supplying water to the urban area, the Kurang and Soan Rivers have been dammed at Rawal and Sambli Lakes, respectively. The quality and quantity of the supply are improved by the vast forest reserves in the Kurang and Soan River headwaters. Ground water is produced principally from Quaternary alluvial gravels by an additional infrastructure of municipal and private wellbores that extends down to 200 meters. The water table drops in elevation from near the Soan River (approximately 450 m) to about 600 m at the foot of the Margala Hills, therefore the saturated zone often sits 2 to 20 meters below the natural surface of the ground (Ashraf and Hanif, 1980). The Lei Nala contributes significantly to the Soan River's pollution below their confluence by transporting the majority of the liquid pollution from Rawalpindi (Sheikh et al., 2007).

4.1.4. General climate

The statistics for the Islamabad station of the Pakistan Department of Meteorology show a monsoonal weather with hot, rainy summers and moderate, dry winters; precipitation is typical of Pakistan's semiarid zone. The monsoon season typically starts in June, maxima in August, and finishes in September. Winter monsoon activity is at its least intense in March. The four-monsoon summertime always have some amount of precipitation, although each of the other months could well be completely dry. Only 249.1 millimeters of rain fell annually in 1982. 1,732 mm was the record high for 1983. From 1931 through 1987, the average rainfall was 1,055 mm. The highest recorded temperature was 45.9 °C in June of 1972, and the coldest was -3.9 ° C in a January prior 1961. The only times that freezing temperatures have been recorded are in the months of November, December, and January. Snow has never occurred here. ("Pakistan Department of Meteorology", 1988; Sheikh et al., 2007).

4.2. Pattern of Land Use and Land Cover Changes (LULC)

4.2.1. 1990

Landsat imagery and supervised classification technique was used to produce patterns of LULC changes for the study area. Images were classified in to five classes

namely water, barren, vegetation, forest, and settlement. Accuracy assessment was done as well as the area of each class was calculated as shown in the table below.

As shown in the table 5, the total area for water, barren, vegetation, forest and urban for the year 1992 in square kilometer is 50 km², 2630 km², 1452 km², 1596 km², and 382 km² respectively with area percentage for each class being 0.82%, 43.04%, 23.76%, 26.12% and 6.25% respectively.

The results for the year 1990 in table 5 and table 6 show that the class that covered the major area of our study area was barren with area percentage being 43.04% (2630 km²) followed by vegetation cover having an area percentage of 23.76% (1452 km²). The class that has covered the least area is water with an area percentage of 0.82% (50 km²) followed by settlement class having an area percentage of 6.25% (382 km²).

According to the figure 4, which is showing the LULC map of 1990, the light green color shows vegetation which is spread all over the study area but is concentrated mostly the area between 33°0'0" N -33°20'0" N, 73°0'0" E-74°0'0" E. The barren class is shown in the figure by a dark brown color. This class is majorly concentrated in the eastern and southeastern border of the study area i.e., between 33°0'0" N-33°2'0"N and 73°0'0" E-73°20'0" E. The forest class is represented by a dark green color in fig 14 the forest in the study area is majorly present in the north between 33°40'0" N-34°0'0"N and 73°40'0" E-74°0'0"E. Water in the study area is shown with a blue color. According to the map there are few recognizable water bodies in the study area. The major water body is the Soan river running through the Potohar region which is 250 km long. Another water body is present in the Islamabad region of the study area namely Rawal lake at 33° 42' 9.58" N and 73° 7' 33.98" E. The extreme southeastern border of the map also shows a blue color marking water of the Jhelum River. Last one is the class of urban/settlement area that is represented by a white color. The urban class is mostly spreads in the upper half of the study area with major concentration between 33°20'0" N-33°40'0"N and 73°00'0"E-73°20'0" E.

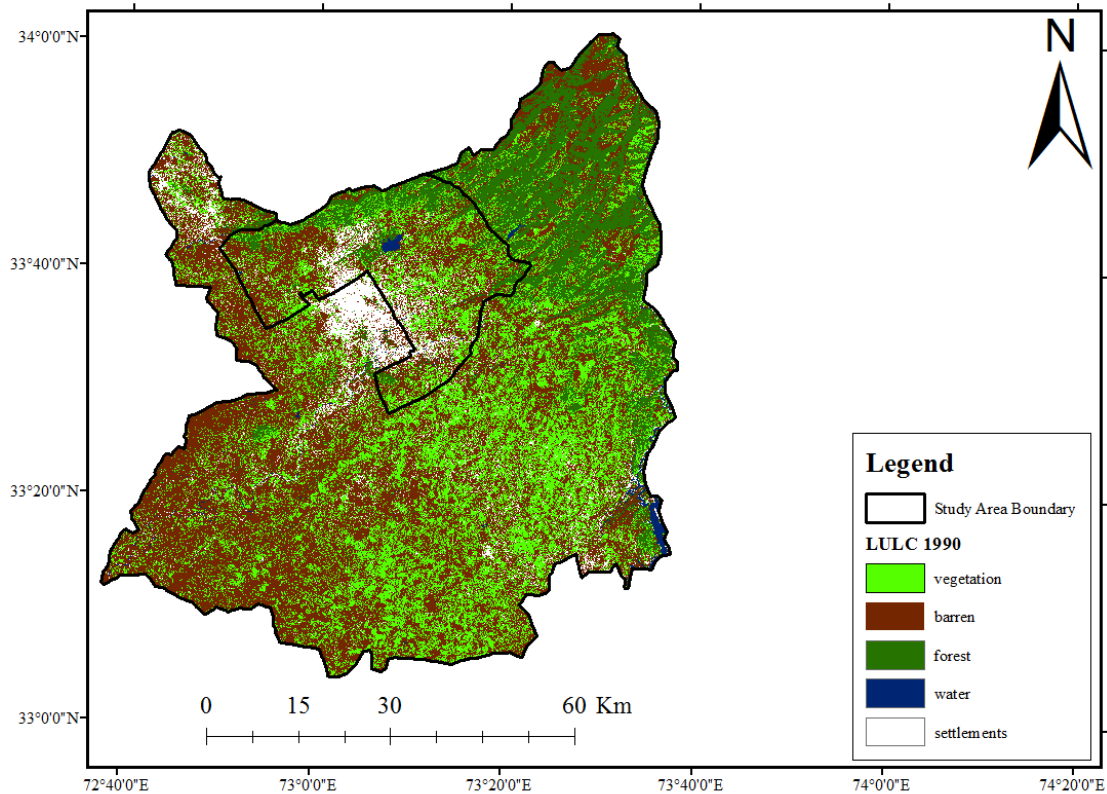


Figure 4.4: LULC 1990

4.2.2. 2000

The year 2000 was a drought year, as the drought started from 1997 and ended in 2001. The year 2000 was the highest peak point of the drought (Hussain, 2011). A lot of changes have been observed in the year 2000.

The following changes in land in Kilometer Square has been observed, as shown in the table 5:

- The total area of water bodies has changed from 50 km² in 1990 to 23 km² in 2000.
- The total area of barren has changed from 2630 km² in 1990 to 2803 km² in 2000.
- The total area of vegetation has changed from 1452 km² in 1990 to 1231 km² in 2000. This year had the least amount of vegetation when compared to other 3 decades.
- The total area of forest has changed from 1596 km² in 1990 to 1464 km² in 2000.
- The total area of settlement has changed from 382 km² in 1990 to 589 km² in 2000.

The following changes by percentage has been observed, as shown in the table 6 (negative values indicated decrease whereas the positive values indicate increase):

- The percentage of Water body has decreased by -54.00% as compared to 1990.
- The percentage of Barren has increased by +6.58% as compared to 1990.
- The percentage of Vegetation has decreased by -15.22% as compared to 1990.
- The percentage of Forest has decreased by -8.27% as compared to 1990.
- The percentage of Settlement has decreased by -54.19% as compared to 1990.

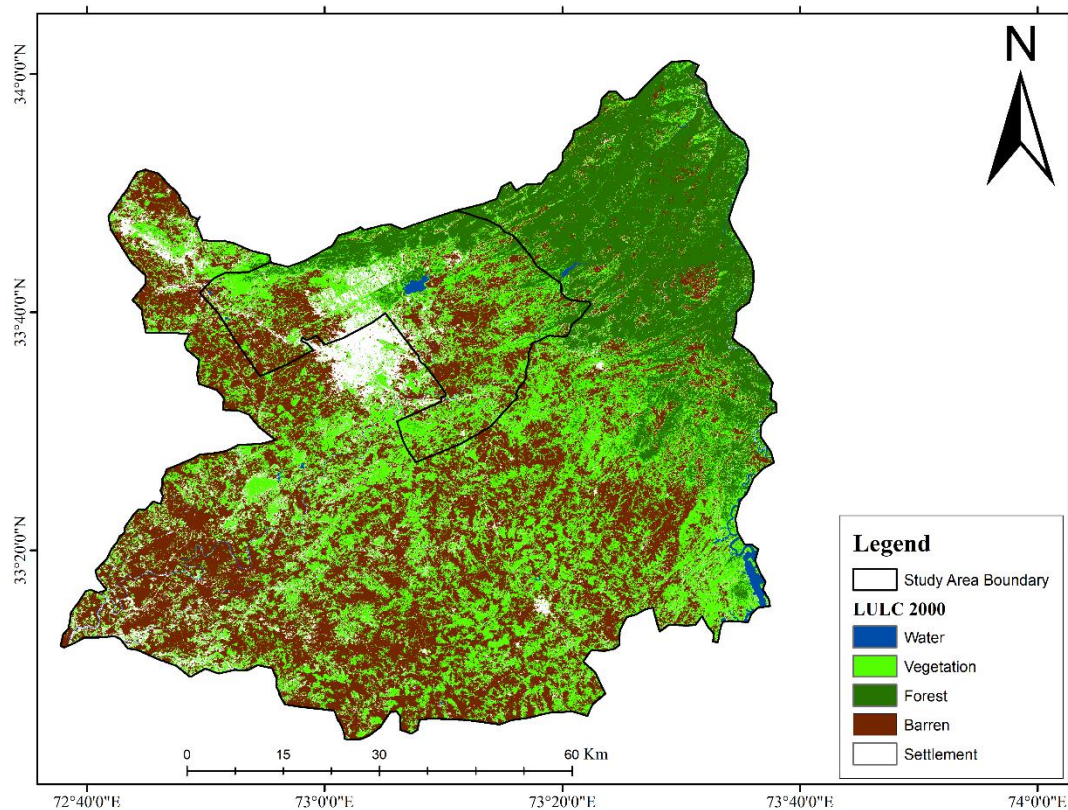


Figure 4.5: LULC 2000

4.2.3. 2010

According to the findings of LULC in 2010, the top northeast of the map shows that there is an increase in barren area on the northern parts with compared to 2000, whereas if we compare it with 1990, we see a decrease in barren area from 2010 to 1990 this is mostly due to the decrease in deforestation and The Forest Act. The following changes in land in Kilometer Square has been observed, as shown in the table 5:

- The total area of water bodies has changed from 23 km² in 2000 to 27 km² in 2010.
- The total area of barren has changed from 2803 km² in 2000 to 2660 km² in 2010. Thus, barren has decreased by 143 km².
- The total area of vegetation has changed from 1231 km² in 2000 to 1333 km² in 2010. So, there is a slight increase in the vegetation cover land.
- The total area of forest has changed from 1464 km² in 2000 to 1284 km² in 2010. This year had the least amount of forest cover land as compared to other three decades.
- The total area of settlement has changed from 382 km² in 1990, 589 km² in 2000 and, 706 km² in 2010 to 923 km² in 2021. So, there is a linear increase in the urban land over the years.

The following changes by percentage has been observed, as shown in the table 6 (negative values indicated decrease whereas the positive values indicate increase):

- The percentage of Water body has increase by +57.73% in 2021 as compared to +17.39% in 2010 and -54.00% decrease in 2000 when compared to 1990.
- The percentage of Barren land has decreased by -21.07% in 2021 as compared to -5.10% in 2010 and +6.56% increase in 2000 when compared to 1990.
- The percentage of Vegetation has increased by +26.13% in 2021 as compared to +8.29% in 2010 and -15.22% decrease in 2000 when compared to 1990.
- The percentage of Forest area has increased by +6.26% in 2021 as compared to -12.30% in 2010 and -8.27% decrease in 2000 when compared to 1990.
- The percentage of Settlement has increased by +30.67% in 2021 as compared to +19.86% in 2000, and +54.19% increase in 2000 when compared to 1990.

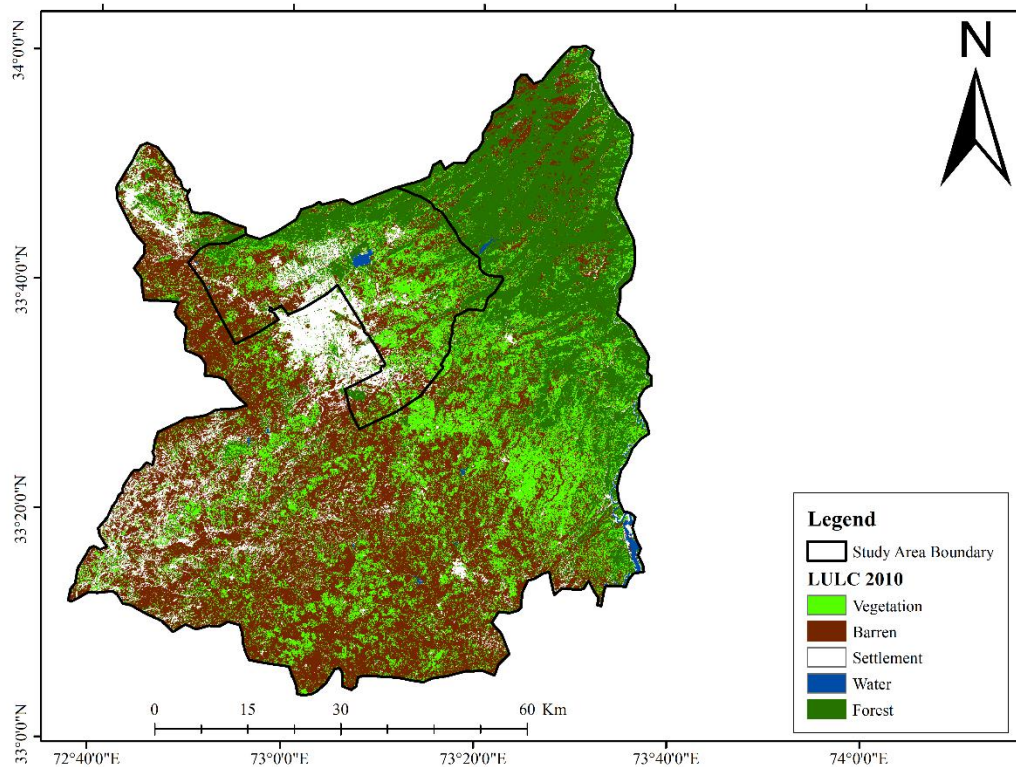


Figure 4.6: LULC 2010

4.2.4. 2021

The latest year of map classification was also the most accurate classification. That is year 2021. This is mainly due to the increase in the quality of satellite imagery. The biggest change has occurred in settlement, with also decrease in forest land cover. The following changes in land in Kilometer Square has been observed, as shown in the table 5:

- The total area of water bodies has changed from 50 km² in 1990, 23 km² in 2000 and, 27 km² in 2010 to 43 km² in 2021.
- The total area of barren has changed from 2630 km² in 1990, 2803 km² in 2000 and, 2660 km² in 2010 to 2099 km² in 2021. Thus, overall, it has decreased since 1990. Also, this year had the least amount of barren when compared to other 3 decades.
- The total area of vegetation has changed from 1452 km² in 1990, 1231 km² in 2000 and, 1333 km² in 2010 to 1681 km² in 2021. So, there is an increase in the vegetation cover land. Also, that this year had the maximum area of land covered in vegetation.

- The total area of forest has changed from 1596 km² in 1990, 1464 km² in 2000 and, 1284 km² in 2010 to 1364 km² in 2021. Though, it has decreased dramatically as compared to year 1990, over the year the forest cover has increased when compared to 2010.
- The total area of settlement has changed from 382 km² in 1990, 589 km² in 2000 and, 706 km² in 2010 to 923 km² in 2021. So, there is a linear increase in the urban land over the years.

The following changes by percentage has been observed, as shown in the table 6 (negative values indicated decrease whereas the positive values indicate increase):

- The percentage of Water body has increase by +57.73% in 2021 as compared to +17.39% in 2010 and -54.00% decrease in 2000 when compared to 1990.
- The percentage of Barren land has decreased by -21.07% in 2021 as compared to - 5.10% in 2010 and +6.56% increase in 2000 when compared to 1990.
- The percentage of Vegetation has increased by +26.13% in 2021 as compared to +8.29% in 2010 and -15.22% decrease in 2000 when compared to 1990.
- The percentage of Forest area has increased by +6.26% in 2021 as compared to - 12.30% in 2010 and -8.27% decrease in 2000 when compared to 1990.
- The percentage of Settlement has increased by +30.67% in 2021 as compared to +19.86% in 2000, and +54.19% increase in 2000 when compared to 1990.

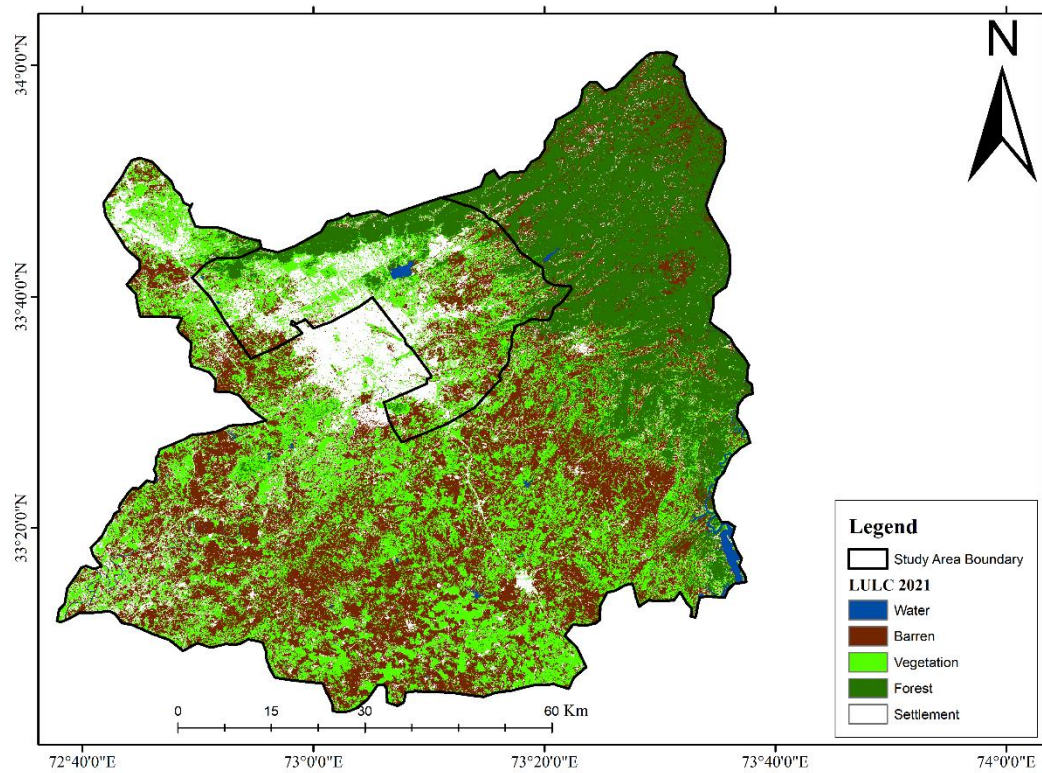


Figure 4.7: LULC 2021

4.2.5. Decade-wise LULC area for each class

Table 4.5: LULC area per decade

Feature	1990	2000	2010	2021
	Km²	Km²	Km²	Km²
Water	50	23	27	43
Barren	2630	2803	2660	2099
Vegetation	1452	1231	1333	1681
Forest	1596	1464	1284	1364
Settlement	382	589	706	923
Total	6110.00	6110.00	6010.00	6110.27

4.3. Net change in LULC

The patterns of LULC were derived by using Landsat data and classifying them into different classes as shown in the feature column of table 6. For the year 2000 the change in water, barren, vegetation, forest and settlement as compared to 1990 is -27 km² (-54%), 173 km² (6.58%), -221 km² (-15.22%), -132 km² (-8.27%), 207 km² (54.19%) respectively and for the year 2010 in comparison to year 2000 the changes in water, barren, vegetation, forest and settlement is 4 km² (17.39%), -143 km² (-5.10%), 102 km² (8.29%), -180 km² (-12.30%), 117km² (19.86%) respectively. For the year 2021, the changes in water, barren, vegetation, forest, and settlement in comparison to year 2010 is 15.59km² (57.73%), negative (-)560.53 km² (-21.07%), 348.30km² (26.13%), 80.41km² (6.26%), 216.51 km² (30.67%) respectively.

The net changes in area from the year 1990-2021 in water, barren, vegetation, forest, and settlement classes is -7.412 km² (-14.82%), -530.53 km² (-20.17%), 229.30 km² (15.79%), negative (-)231.59 km² (-14.51%), 540.51 km² (141.49%) respectively.

From the data shown in the table 6, the water, barren and forest had an overall negative net change from 1990-2021 while the settlement and vegetation had a positive net change.

The minimum change in water, barren, vegetation, and settlement classes was in the year 2010, while for the forest class the minimum percentage change in the year was in the year 2021. The maximum change in area percentage for water, barren, and vegetation classes were in the 2021. For the forest and settlement classes, the maximum increase in area percentage was in the year 2010 and 2000 respectively.

Comparing the overall net change for all the classes from 1990-2021, the maximum net change in area percentage was for the settlement class that had an increase of 141% followed by barren class that had an increase rate of 20%, while the minimum overall net change for the same time span was for the forest class that had an increase of only 14.5% followed by water that had an increase of 14.8% only.

Table 4.6: Net changes in LULC

Feature	2000		2010		2021		Net Changes	
	Change (km2)	% Change	Change (km2)	% Change	Change (km2)	% Change	Change (km2)	% Change
Water	-27	-54.00	4.00	17.39	15.59	57.73	-7.412	-14.82
Barren	173	6.58	-143.00	-5.10	-560.53	-21.07	-530.53	-20.17
Vegetation	-221	-15.22	102.00	8.29	348.30	26.13	229.30	15.79
Forest	-132	-8.27	-180.00	-12.30	80.41	6.26	-231.59	-14.51
Settlement	207	54.19	117.00	19.86	216.51	30.67	540.51	141.49

4.4. Accuracy assessment

According to the steps explained in the sub-topic 3.4., we assessed the accuracy of LULC maps from 1990 to 2021, the overall accuracy of year 1990, 2000, 2010, and 2021 is 70.42%, 74.44%, 71.04%, and 84.59% respectively. The User's accuracy of year 1990, 2000, 2010, and 2021 is 71.99%, 75.45%, 70.52%, and 85.85% respectively. The producer's accuracy of year 1990, 2000, 2010, and 2021 is 71.74%, 76.63%, 70.71%, and 83.94% respectively.

Table 4.7: Accuracy assessment of Land Use and Land Cover

Year	User Accuracy (%)	Producer Accuracy (%)	Overall Accuracy (%)
1990	71.99	71.74	70.42
2000	75.45	74.63	74.44
2010	70.52	70.71	71.04
2021	85.82	83.94	84.59

4.5. Accuracy assessment points

50 points on Google Earth Pro were taken for each decade for the purpose of accuracy assessment as shown in figure below:

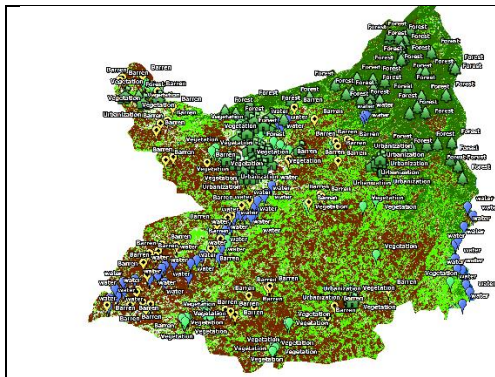


Figure 4.8: Assessment points of year 1990

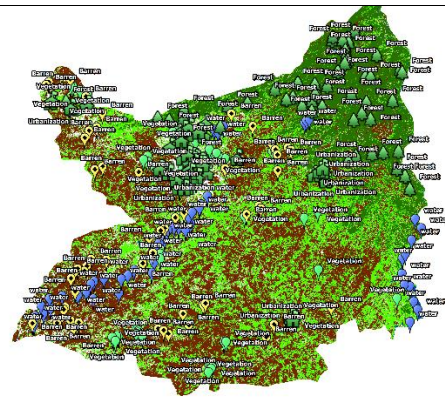


Figure 4.9: Assessment points of year 2000

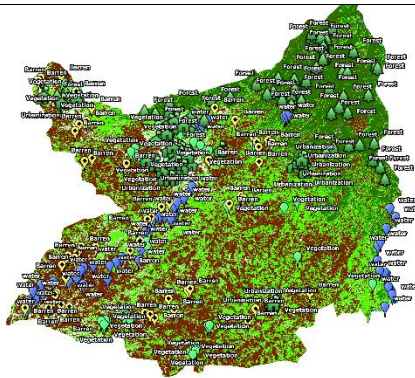


Figure 4.10: Assessment points of year 2010

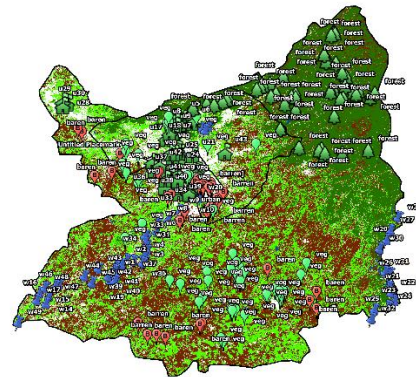


Figure 4.11: Assessment points of year 2021

4.6. Pattern of Land Surface Temperature (LST) changes

4.6.1. 1990

The LST patterns for study area are derived from Landsat thermal bands which are then ran through different equations. The figure 12 shows the map of study area representing land surface temperatures of the year

According to the map, five classes of temperatures are represented through different colors. The area with temperature less than or equal to 10°C, between 10°C to 15°C, between 15°C to 20°C, between 20°C to 25°C and above 25°C represented by dark green, light green, yellow orange, and red color respectively. The dominant colors on the map as shown in the figure 12 are light green (10-15°C) followed by yellow (15-20°C) with patches

of dark green ($\leq 10^{\circ}\text{C}$) in the areas of higher altitude of the study area. For the year 1992, there is no area that has a land surface temperature above 25°C .

The part of the area under study that has a temperature less than or equal to 10°C , $10-15^{\circ}\text{C}$, $15-20^{\circ}\text{C}$, $15-20^{\circ}\text{C}$ and above 25°C has an area percentage of 4.66%, 74.70%, 20.57%, 0.07% and 0% respectively.

The central part of the map is majorly under the temperature range of $10-15^{\circ}\text{C}$ with the southwest of the study area along the borders is under the temperature range of $15-20^{\circ}\text{C}$. The north eastern part has high altitude mountain ranges that has patches of green showing land surface temperature to be less than or equal to 10°C but the extreme top north eastern corner shows temperature to be between $15-20^{\circ}\text{C}$ because of deforestation. In the same location that is the top corner of the north eastern side there are small patches of orange in the middle of yellow ($15-20^{\circ}\text{C}$) showing specific areas having temperatures above than the neighboring areas because of the presence of barren land.

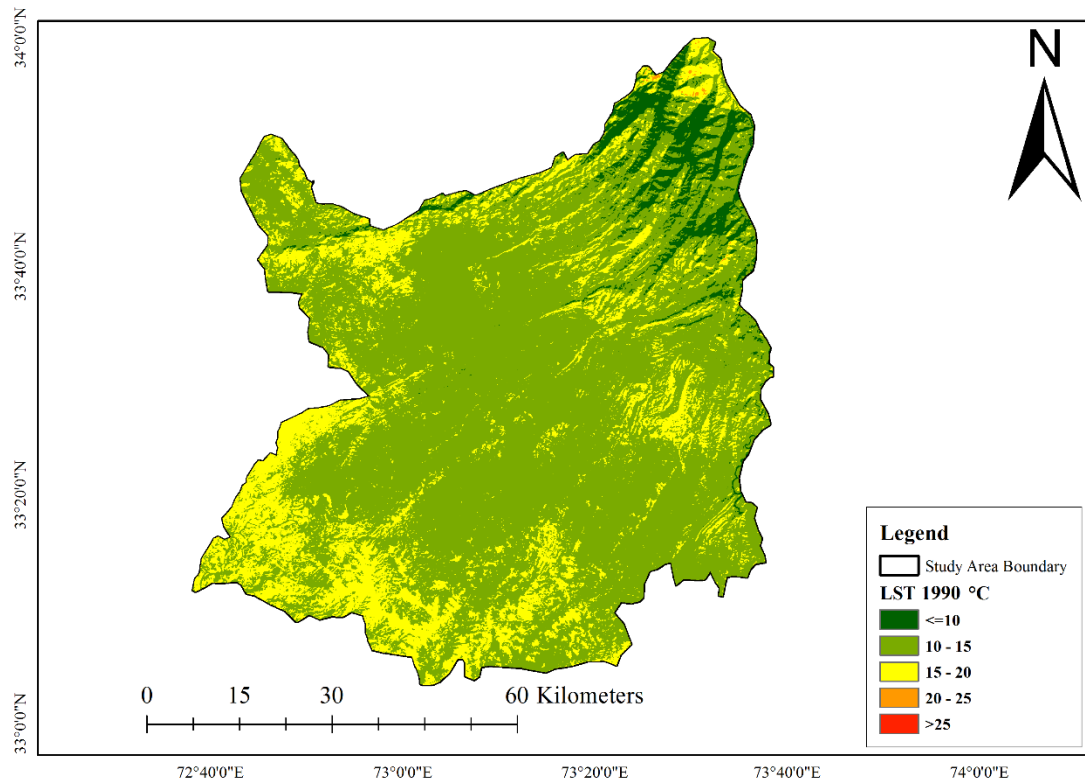


Figure 4.12: LST 1990

4.6.2. 2000

According to the findings of LST of 2000, shown in table 9, the highest temperature is risen to 37.22°C from previously 23.68°C in 1990. The lowest temperature has increased from 1.89°C to 10.52°C. The overall changes in the lower and the higher temperature were observed to be 8.63°C and 13.54°C respectively.

The year 2000 was a drought year, meaning that the temperature was higher than usual. As shown in the figure 13, almost the whole map is covered in red, which shows that the temperature everywhere was higher than 25°C. Even in the high altitudes, the temperature was from 15°C range to 25°C. Only a small fraction of the area of high altitudes can be seen to be somewhere between 10°C to 15°C. The main city of Islamabad, below the foot of Margalla hills, the temperature is in orange, indicating ranges from 20°C to 25°C while Rawalpindi has only a few areas of orange range. This is mainly because the city of Islamabad has much more vegetation cover than Rawalpindi, where the later only has vegetation in few areas, like Ayub Park and Jinnah Park. The temperature of Margalla hills and the foot of the Himalaya is almost the same, the orange range of 20°C-25°C, even in the month of November.

Table 4.8: LST 2000 (low, high, and net changes in temperature)

Lower T(°C) (1990)	Higher T(°C) (1990)	Lower T(°C) (2000)	Higher T(°C) (2000)	Net Change in Lower T(°C)	Net Change in higher T(°C)
1.89	23.68	10.52	37.22	8.63	13.54

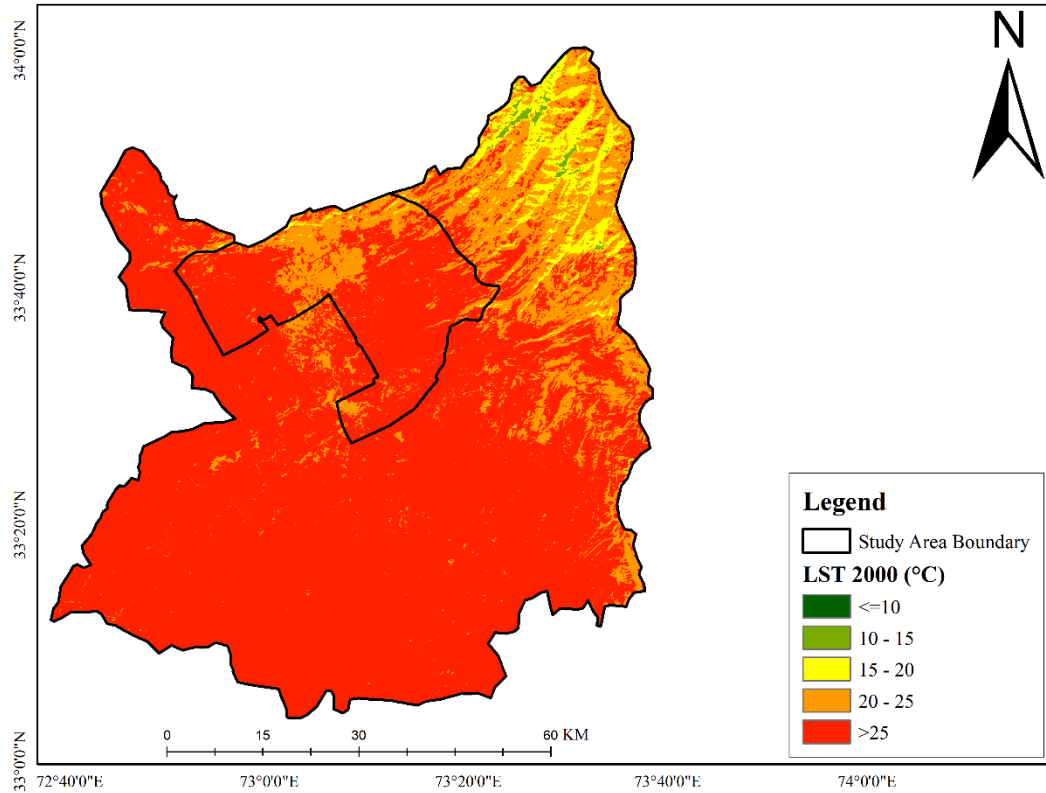


Figure 4.13: LST 2000

4.6.3. 2010

According to the findings of LST of 2011, shown in figure 14 and values in table 8 and 9, the highest temperature is decreased to 34.36°C from previously 23.68°C in 1990. The lowest temperature has increased to 9.98°C in 2010 from 1.89°C in 1990. The reason for higher temperature in the previous decade is that the year 2000 was a drought year. Now, after the drought year the temperature has decreased overall in the main city portion of the twin cities from 2000 to 2010 but still the temperatures have increased from 1990 to 2010 due to gradual increase in urbanization, climate change and other anthropogenic activities, but the top Northeastern part has again seen increase in temperature.

The bottom part of the map, as according to the figure 14, there is a big patch of high temperature, which is in according to the figure 6, the LULC of 2010, there is big patch of barren land there, which explains the high temperature value. Surprisingly, when compared to the figure 4, we can see that the city of Islamabad and Rawalpindi lies around the range of 10 to 15 degree centigrade. The top left part of 'Wah cantt' has also patches

of 10 to 15 degrees centigrade but it also has patches of 15 to 20 degrees, which according to the figure 14, is again due to the presence of barren land.

Table 4.9: LST 2010 (Low, high, and net change in temperature)

Lower T(°C) (2000)	Higher T(°C) (2000)	Lower T(°C) (2010)	Higher T(°C) (2010)	Net Change in Lower T(°C)	Net Change in higher T(°C)
10.52	37.22	9.98	34.36	-0.54	-2.86

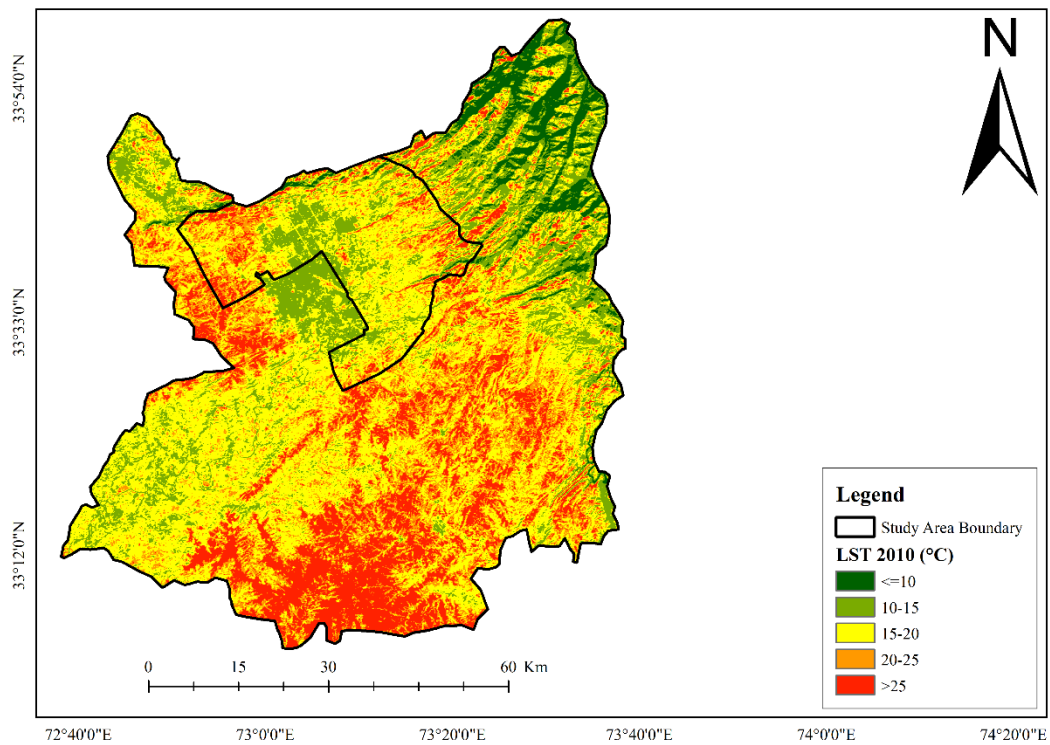


Figure 4.14: LST 2010

4.6.4. 2021

According to the findings of LST of 2021, shown in table 10, the highest temperature is risen to 35.49°C from 34.36°C in 1990. The lowest temperature has increased from 9.98°C to 15.61°C. The overall changes in the lower and the higher temperature were observed to be 5.63°C and 1.13°C respectively.

As shown in the figure 15, the Eastern part of the city has seen junction of high increase in temperature, this is due to the creation of barren land due to creation of housing societies in that portion. The overall temperature of the main portion of the twin cities has significantly increased, to the point where the streets can be easily distinguished. The main central part of Rawalpindi has seen more intense changes than Islamabad mainly due to less vegetation and increase in cemented urban area. The Northeastern part has seen increase in housing societies, due to which the temperature has significantly risen as these societies require clearing of vegetation and forest covers. The farthest top Northeastern part has again seen increase in temperature. This can be traced to the increase in the urbanization in the higher altitudes.

When comparing the map of figure 15 and figure 7, it can be clearly seen that the areas where barren land has increased, are also the area where the temperature of more than 25 degree centigrade has increased as well. In the top left corner of the map, the increase in urbanization has yet again increased the overall temperature of the area.

Table 4.10: LST 2021 (low, high, and net changes in temperature)

Lower T(°C) (2010)	Higher T(°C) (2010)	Lower T(°C) (2021)	Higher T(°C) (2021)	Net Change in Lower T(°C)	Net Change in higher T(°C)
9.98	34.36	15.61	35.49	5.63	1.13

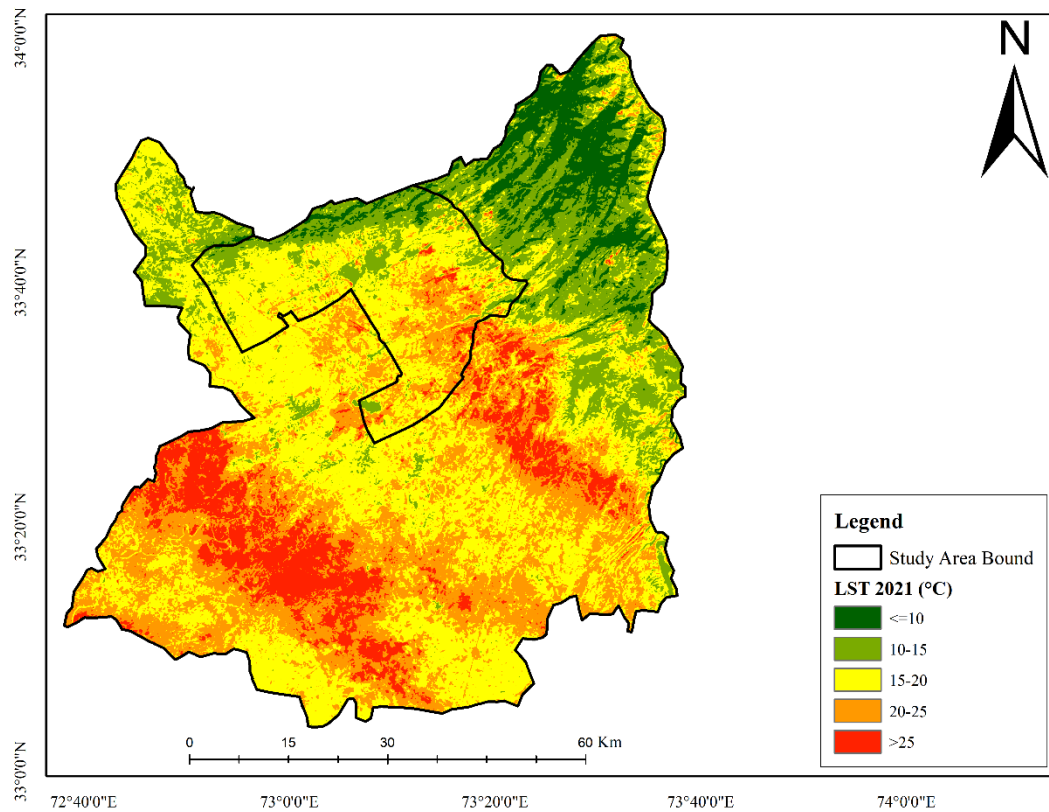


Figure 4.15: LST 2021

4.7. Net Change in LST

Table 4.11: LST net changes in area km² and area Percentage

LST Ranges	Percentage Area 1990	Percentage Area 2000	Percentage Area 2010	Percentage Area 2021
<=10	4.66	0.00	6.43	12.24
10 to 15	74.70	0.31	20.06	15.11
15-20	20.57	3.70	38.80	35.01
20-25	0.07	17.28	24.42	25.20
>25	0.00	78.72	10.34	12.10

Table 4.12: Net changes in LST (degree Centigrade)

Year	Lower T(°C)	Higher T(°C)
1990	1.89	23.68
2000	10.52	37.22
2010	9.98	34.36
2021	15.61	35.49
Net Change	13.72	11.81

The patterns of LST were analyzed by calculating the Thermal, Infra-Red, and red bands using various equations in the past 3 decades (1990-2021), the values of which are shown in the table (11, 12). The lower temperature of from 1990 to 2021 has increased by 13.72°C & the higher temperature has increased by 11.81°C. The highest temperature was observed in the year 2000, which was a drought year, whose area was about 4810 km² and consisted of 78.72% of the total study area.

In comparison to the previous year, 1990, the increase in the percentage area of high temperature (more than 25 degree centigrade) was about a total of whole 78.72%, one of the reasons is that it was a drought year in 2000 but it can also be due to climate change and anthropogenic activities. The net change in the highest temperatures (>25°C) from 1990 to 2021, was 12.10%, as the area percentage in 1990 was 0%. The area with temperature range of 20 to 25 degree centigrade, has increased from 0.07% in 1990 to 25.20% in 2021, which accounts for a net change of 27.49%. The area with temperature range of 15 to 20 degree centigrade, has increased from 20.57% in 1990 to 35.01% in 2021, which accounts for a net change of 14.44%. The area with temperature range of 10 to 15 degree centigrade, has decreased from 74.70% in 1990 to 15.11% in 2021, which accounts for a net change of 59.29%. The area with temperature range of less than or upto 10 degree centigrade, has overall decreased from 4.66% in 1990 to 12.24% in 2021, which accounts for a net change of 7.77%.

With the exception of the year 2000, the temperature range of more than 25 degrees shows an increase trend per decade. The value of temperature from 1990 to 2000 was 0% to 78.72% respectively, but after that it decreases to 10.34% in 2010 and then again shows

an increasing trend by almost 2 percent, that is, 12.10% in the year 2021. The sudden increase in the year 2000 is due to the drought conditions that year (Hussain, 2011). The area with temperature range of 20 to 25 degrees centigrade, shows an increasing trend from 0.07% in 1990 to 17.28%, 24.42% and 25.20% in the year 2000, 2010 and 2021 respectively. The area with temperature range of 15 to 20 degrees centigrade, shows an increasing trend with the exception of the year 2000, where temperature value dropped from 20.57% to 3.70% in 1990 and 2000 respectively. The decrease in temperature is because the higher temperature values, that is above 15-20 degree centigrade, have increased drastically. After the year 2000, there is decreasing trend of 38.80% to 35.01% in 2010 and 2021 respectively. The area with temperature range of 10 to 15 degrees centigrade, shows a decreasing trend, yet again with the exception of the year 2000. The previous decades were colder than the recent ones due to changes in urbanization, deforestation, climate change and anthropogenic activities. The rapid urbanization results in more construction and transformation of vegetation and agriculture land into barren land, leading to further increase in LST, this in return synergizes the effects of global warming, particularly localized urban warming. The value of temperature of 1990, 2000, 2010, and 2021 are 74.70%, 0.31%, 20.06% and 15.11% respectively. The area with temperature range of less than or equal to 10 degrees centigrade has decreased from 1990 to 2000 then increases in 2010 and 2021, their respective values are as follow: 4.66%, 0.00%, 6.43% and 12.24%. The increase in the lower temperature can be accounted for due to the increase in the afforestation.

4.8. Comparison with other studies.

According to the study of Ullah et al. (2019), the results showed that an increase in urbanization by 5.57% and in bare soil by 4.22% while there was a decrease in vegetation cover by 9.88% during 1990-2017.

Khan et al. (2020) conducted a study on LULC and the results showed an increase in built up area by 11.9% in the time span of 26 years. The study reveals that due to the conversion of forests land, waterbodies and vegetation areas into in-built areas has caused a warming effect with a contribution of 1.52 degree Celsius while the conversion of barren land and built-up area into forests or water bodies have contributed to a cooling effect of -

0.85 degree Celsius on relative LST. Hence the positive (warming) contribution to UHIs is higher than negative (cooling) contribution. The study concluded that the LULC induced warming has increased over the region from 1993-2018.

Rahman et al. (2022) conducted a study on Northern Pakhtunkhwa mountainous region of Pakistan for modelling of LULC and LST variations examined 30 years changes in LULC and LST i.e., from 1987-2017. The results of LULC classification showed an increase in built-up area and bare soil classes by 13 km² and 89 km² respectively while there was a decrease in vegetation classes by 144 km² during 1987-2017. For the same time span, for LST, the temperature range increased by 140 km² for the next 30 years i.e., till 2047, the findings show similar trend for each class.

In comparison to these studies, our studies showed an increase in settlement of 541 km² from 1990 to 2021, that is an increase of 141.49%. The vegetation cover also saw an increase in by 15.79%. The barren land saw a decrease by 20.17%, mainly due to increase in agricultural land. For LST, the biggest change occurred in temperature range of twenty to twenty-five degree centigrade, by an increase of percentage area from 0.07% in 1990 to 25.20% in 2021.

Chapter 5 – Conclusion and Recommendation

5.1. Conclusion

This study focused on the assessment and analysis of LULC and LST of the twin city: Islamabad and Rawalpindi, from 1990 to 2021. Assessment was done through the maximum likelihood classification and Thermal Infrared, Red, and Near Infrared bands.

The major visible changes occurred in urbanization land from 1990 to 2021 where the urban area increased from 382 km² to 923 km² in just 10 years. This accounts for increase in rate of urbanization by 141.49%. Due to the increase in the housing societies, and the clearing of the land, it can be predicted that this settlement area will increase more. The vegetation area showed a decrease from 1990 to 2000 but from 2000 to 2021 it increased slightly. This can be mainly due to the increase in the agricultural land. Barren land showed a decreasing trend from 1990 to 2021 except for the year 2000, where it increased due to the emergence of drought year. The higher altitude has seen quite some changes regarding afforestation, deforestation and built up of settlement. The water bodies have shown only a slight change as rivers are seasonal and not perennial. Lastly, in forest area, there is a decreasing trend due to deforestation and urbanization.

Overall, the trend of LST was seen as an increase in temperatures, mainly in the sub-division of temperature from 15 to more than 25°C. The overall net increase in the lowest temperature from 1990 to 2021 was 13.72°C and the net highest temperature was 11.81°C.

5.2. Recommendations

Regarding the unsustainable urban expansion and deforestation, we recommend sustainable urban planning and management in the region. We propose that the Government should revise the policies regarding the urban expansion, boundary and conservation and preservation of forest ecosystem. S

The followings are some other recommendations:

- The analysis of LULC, especially for the early decades of 1990 and 2000, would be more precise and accurate, if the satellite imagery available was of higher resolution and quality. By this the accuracy of LULC would increase and the results would be better.
- The result of LULC can be more precise for the decision and policy makers if the results are compared with ground truthing. Ground truthing or ground survey provides real and true values of each LULC parameter.
- The result of LST values would be more accurate if the weather parameters like humidity and precipitation were included.
- The result of LST only included temperature of one day per month of each decade. The precision would increase if it was averaged for the same season.

References

- Aboelnour, M., & Engel, B. A. (2018). Application of Remote Sensing Techniques and Geographic Information Systems to Analyze Land Surface Temperature in Response to Land Use/Land Cover Change in Greater Cairo Region, Egypt. *Journal of Geographic Information System*, 10(01), 57–88.
- Adeel, M. (2010) ‘Assessing the implementation of Rawalpindi’s Guided Development Plan through GIS and Remote Sensing’, REAL CORP 2010 Proceedings, (May), pp. 18–20.
- Ahmad, Sheikh & Abbasi, Q. & Jabeen, Rukhsana & Shah, Muhammad. (2012). Decline of Conifer Forest cover in Pakistan: A GIS approach. *Pakistan Journal of Botany*. 44. 511-514.
- Akram Kahlown, M., & Majeed, A. Water-Resources in Pakistan: Challenges and Future Strategies. *Sciencevision.org.pk*.
- Alberto Franco-Solís, Claudia V. Montaña, Dynamics of deforestation worldwide: A structural decomposition analysis of agricultural land use in South America, *Land Use Policy*, Volume 109, 2021, 105619, ISSN 0264-8377.
- Ali Khan, S., & Naseem Baig, M. (2013). The Linkage between Agricultural Practices and Environmental Degradation. *Jett.dormaj.com*.
- Allen, J.C. and Barnes, D.F. (1985), The Causes of Deforestation in Developing Countries. *Annals of the Association of American Geographers*, 75: 163-184.
- Attri, P., Chaudhry, S. And Sharma, S. (2015) ‘Remote Sensing & GIS based Approaches for LULC Change Detection - A Review’, *International Journal of Current Engineering and Technology*, 5(5), pp. 3126–3137.
- Avinash Kumar Ranjan, Akash Anand, Patibandla B. Sravan Kumar, Santosh Kumar Verma, Lakhindar Murmu. Prediction of Land Surface Temperature Using Artificial Neural Network in Conjunction with Geoinformatics Technology Within Sun City Jodhpur (Rajasthan), India.
- Azam, A., & Shafique, M. (2017). Agriculture in Pakistan and its Impact on Economy—A Review. *International Journal Of Advanced Science And Technology*, 103, 47-60.
- Babur, Z., Ali, A., & Naseem Baig, M. (2013). Desertification in Pakistan, Challenges and Opportunities. *Jett.dormaj.com*.
- Becker, F., & Li, Z. (1995). Surface temperature and emissivity at various scales: Definition, measurement, and related problems. *Remote Sensing Reviews*, 12(3-4), 225-253.
- Bill, R. (2018) ‘Remote sensing and GIS’, *gis.Science - Die Zeitschrift fur Geoinformatik*, (2), p. I.
- Blaschke, T., Hay, G. J., Weng, Q., & Resch, B. (2011). Collective Sensing: Integrating Geospatial Technologies to Understand Urban Systems—An Overview. *Remote Sensing*, 3(8), 1743–1776. MDPI AG.
- Bongaarts, J., & Casterline, J. (2013). Fertility Transition: Is sub-Saharan Africa Different? *Population and Development Review*, 38, 153–168.
- Boxall AB, Kolpin DW, Halling-Sørensen B, Tolls J. Are veterinary medicines causing environmental risks? *Environ Sci Technol*. 2003 Aug 1;37(15):286A-294A.

- Braud, I., Dantas-Antonino, A., & Vauclin, M. (1995). A stochastic approach to studying the influence of the spatial variability of soil hydraulic properties on surface fluxes, temperature and humidity. *Journal Of Hydrology*, 165(1-4), 283-310.
- Brunsell, N., & Gillies, R. (2003). Length Scale Analysis of Surface Energy Fluxes Derived from Remote Sensing. *Journal Of Hydrometeorology*, 4(6), 1212-1219.
- Chander, G., Markham, B. L. And Helder, D. L. (2009) ‘Summary of current radiometric calibration coefficients for Landsat MSS, TM, ETM+, and EO-1 ALI sensors’, *Remote Sensing of Environment*, 113(5), pp. 893–903.
- Chang, Y., Hou, K., Li, X., Zhang, Y., & Chen, P. (2018). Review of Land Use and Land Cover Change research progress. *IOP Conference Series: Earth And Environmental Science*, 113, 012087.
- Cillis, G., Tucci, B., Santarsiero, V., Nolè, G., & Lanorte, A. (2021). Understanding Land Changes for Sustainable Environmental Management: The Case of Basilicata Region (Southern Italy). *Pollutants*, 1(4), 217-233.
- Clip (analysis)—arcgis pro | documentation. Pro.arcgis.com. (2022). Retrieved 18 august 2022. Retrieved 18 August 2022, from <https://pro.arcgis.com/en/pro-app/2.8/tool-reference/analysis/clip.htm>.
- Composite bands (data management)—arcgis pro | documentation. Pro.arcgis.com. (2022). Retrieved 18 August 2022, from <https://pro.arcgis.com/en/pro-app/2.8/tool-reference/data-management/composite-bands.htm>.
- Convention on Biological Diversity. (2022). Definitions. CBD.int. Retrieved 30 November 2006. Retrieved 30 November 2006, from <https://www.cbd.int/forest/definitions.shtml>.
- Debele, T. A., Adugna, G. M., Bao, P. Q., & Tran, A. D. (2021). Modelling and Accessing Land Degradation Vulnerability using Remote Sensing Techniques and the Analytical Hierarchy Process Approach Modelling and accessing land degradation vulnerability using remote sensing techniques and Abebe Debele Tolche, Megersa A. *Geocarto International*, 0(0), 1–21.
- Defries, R., & Townshend, J. (1994). Ndvi-Derived Land Cover Classifications At A Global Scale. *International Journal Of Remote Sensing*, 15(17), 3567-3586.
- Dennehy, K., Litke, D., & mcmahon, P. (2002). The High Plains Aquifer, USA: groundwater development and sustainability. Geological Society, London, Special Publications, 193(1), 99-119.
- Dynamics of Land-Use and Land-Cover Change in Tropical Regions. Eric F. Lambin, Helmut J. Geist, Erika Lepers. *Annual Review of Environment and Resources* 2003 28:1, 205-241
- Erik Lichtenberg, Chapter 23 Agriculture and the environment, *Handbook of Agricultural Economics*, Elsevier, Volume 2, Part A, 2002, Pages 1249-1313, ISSN 1574-0072, ISBN 9780444510808.
- Esen, Esin & Uslu, Orhan. (2008). Assessment of the effects of agricultural practices on non-point source pollution for a coastal watershed: A case study Nif Watershed, Turkey. *Ocean & Coastal Management - ocean coast manage*. 51. 601-611.

- Extract by mask (spatial analyst)—arcgis pro | documentation. Pro.arcgis.com. (2022). Retrieved 18 August 2022, from <https://pro.arcgis.com/en/pro-app/2.8/tool-reference/spatial-analyst/extract-by-mask.htm>.
- FAO production yearbook 1977. (V. 31). "FAO-Access.No.--41201; 116 tables; Chinese version issued separately."
- Food and Agriculture Organization of the United Nations. 2005. Global Forest resources assessment 2005 thematic study on mangroves. Italy.
- Gergely Toth, Cecília Szigeti, The historical ecological footprint: From over-population to over-consumption, *Ecological Indicators*, Volume 60, 2016, Pages 283-291, ISSN 1470-160X.
- Ghafoor, G. Z., Sharif, F., Shahid, M. G., Shahzad, L., Rasheed, R., & Khan, A. U. H. (2022). Assessing the impact of land use land cover change on regulatory ecosystem services of subtropical scrub forest, Soan Valley Pakistan. *Scientific Reports*, 12(1), 1-12.
- Grooten, M.; Almond, R. E. A. 2018. Living planet report - 2018: aiming higher 2018 pp.148 pp. Ref.25.
- Haider, Sajjad. 2021. "Climate Change 1 Analysis Article." (April).
- Hassan, Z., Shabbir, R., Ahmad, S. S., Malik, A. H., Aziz, N., Butt, A., & Erum, S. (2016). Dynamics of land use and land cover change (LULCC) using geospatial techniques: a case study of Islamabad Pakistan. *SpringerPlus*, 5(1), 1-11.
- Hussain, B., 2022. History of drought in Pakistan – In detail. [online] Pakistan Weather Portal (PWP).
- Hussain, S., Mubeen, M., Ahmad, A., Akram, W., Hammad, H. M., Ali, M., ... & Nasim, W. (2020). Using GIS tools to detect the land use/land cover changes during forty years in Lodhran district of Pakistan. *Environmental Science and Pollution Research*, 27(32), 39676-39692.
- Hussain, S., Mubeen, M., Ahmad, A., Akram, W., Hammad, H. M., Ali, M., Masood, N., Amin, A., Farid, H. U., Sultana, S. R., Fahad, S., & Wang, D. (2020). Using GIS tools to detect the land use / land cover changes during forty years in Lodhran District of Pakistan. 39676–39692.
- Igor A. Shiklomanov (2000) Appraisal and Assessment of World Water Resources, *Water International*, 25:1, 11-32.
- Imen, g., halima, g., & djamel, a. (2022). Relationship between lulc characteristic and lst using remote sensing and gis, case study guelma (algeria) relationship between lulc characteristic and lst using. March.
- Indarto, Jarot, An overview of theoretical and empirical studies on deforestation (2016). *Journal of International Development and Cooperation*.
- James Zollweg, Joseph C. Makarewicz. Detecting effects of Best Management Practices on rain events generating nonpoint source pollution in agricultural watersheds using a physically based stratagem. *Journal of Great Lakes Research*, Volume 35, Supplement 1, 2009, Pages 37-42, ISSN 0380-1330.
- Jarot Indarto and Dadang J. Mutaqin, An Overview of Theoretical and Empirical Studies on Deforestation.

- Jat, M., Khare, D., Garg, P., & Shankar, V. (2009). Remote sensing and GIS-based assessment of urbanisation and degradation of watershed health. *Urban Water Journal*, 6(3), 251-263.
- Jiang, L., Hardee, K. How do Recent Population Trends Matter to Climate Change? *Popul Res Policy Rev* 30, 287–312 (2011).
- Jie Li, Qian Liu, Yao Sang, Several Issues about Urbanization and Urban Safety, *Procedia Engineering*, Volume 43, 2012, Pages 615-621, ISSN 1877-7058.
- Jiyuan, L. I. U., Mingliang, L. I. U., Xiangzheng, D., J, Z. D., Zengxiang, Z., & I, L. U. O. Di. (2002). The land use and land cover change database and its relative studies in China. 3, 275–282.
- Journal Article. 2012. 92-5-000587-3. "Annuaire FAO de la production 1977 (V. 31). Anuario FAO de produccion 1977 (V. 31)."
- Julie Trottier. (2008) Water crises: political construction or physical reality? *Contemporary Politics* 14:2, pages 197-214.
- K. Alan Kronstadt, Pervaze A. Sheikh, Bruce Vaughn, 2010. Flooding in Pakistan: Overview and Issues for Congress. Congressional Research Service.
- Kassas, M., Ahmad, Y., Rozanov, B. Desertification and drought: an ecological and economic analysis. Issue: 20. Pages: 19-29.
- Khan, M. S., Ullah, S., Sun, T., Rehman, A. U. R., & Chen, L. (2020). Land-Use / Land-Cover Changes and Its Contribution to Urban Heat Island: A Case Study of.
- Konikow, L.F., Kendy, E. Groundwater depletion: A global problem. *Hydrogeol J* 13, 317–320 (2005).
- Kustas, W., & Norman, J. (1996). Use Of Remote sensing for evapotranspiration monitoring over land surfaces. *Hydrological Sciences Journal*, 41(4), 495-516.
- Lambin, E., Geist, H., & Lepers, E. (2003). Dynamics of Land-Use and Land-Cover Change in Tropical Regions. *Annual Review Of Environment And Resources*, 28(1), 205-241.
- Landsat 4. Eos. (2022). Retrieved 18 august 2022. Retrieved 18 August 2022, from <https://eos.com/find-satellite/landsat-4-tm/>.
- Landsat 8. Eos. (2022). Retrieved 18 august 2022. Retrieved 18 August 2022, from <https://eos.com/find-satellite/landsat-8/>.
- Landst 5. Eos. (2022). Retrieved 18 august 2022. Retrieved 18 August 2022, from <https://eos.com/find-satellite/landsat-5-tm/>.
- Li, Z., & Duan, S. (2018). Land Surface Temperature. *Comprehensive Remote Sensing*, 264-283.
- Liang, S., and Wang, J. 2020. Advanced Remote Sensing: Terrestrial Information Extraction and Applications. ScienceDirect.
- Liu, C., Stepanov, S., Gott, A., Shields, P. A., Zhirnov, E., Wang, W. N., ... & Zettler, J. T. (2006). High temperature refractive indices of GaN. *physica status solidi c*, 3(6), 1884-1887.
- M. Gurbuz. Qevre Tarimiliskileri , Ziraat Dunyasi Dergisi, Turkiye Ziraatgilar Dernegi Yayinlari. 1992, Sayi: 411.
- M. Kassas, Desertification: A general review, *Journal of Arid Environments*, Volume 30, Issue 2, 1995, Pages 115-128, ISSN 0140-1963.

- Macrotrends.net. 2022. Rawalpindi, Pakistan Metro Area Population 1950-2022. [online] Available at: <https://www.macrotrends.net/cities/22054/rawalpindi/population>. Accessed 8 September 2022.
- Maja, M.M., Ayano, S.F. The Impact of Population Growth on Natural Resources and Farmers' Capacity to Adapt to Climate Change in Low-Income Countries. *Earth Syst Environ* 5, 271–283 (2021).
- Marianne Kjellén And Gordon Mcgranahan. Comprehensive assessment of the freshwater resources of the world. Stockholm environment institute. 1997.
- Marsh, G. P. 1874. *Man and nature: The Earth as modified by human actions*, New York: Scribner Armstrong and Co.
- Mcgrane, S. (2016). Impacts of urbanisation on hydrological and water quality dynamics, and urban water management: a review. *Hydrological Sciences Journal*, 61(13), 2295-2311.
- Mcmillin, L. (1975). Estimation of sea surface temperatures from two infrared window measurements with different absorption. *Journal Of Geophysical Research*, 80(36), 5113-5117.
- Middleton, Nick.; Thomas, David; UNEP. 1992. *World atlas of desertification*. 69 p.
- Mittal, Ishwar and Gupta, Ravi Kumar, *Natural Resources Depletion and Economic Growth in Present Era* (September 30, 2015). SOCH- Mastnath Journal of Science & Technology (BMU, Rohtak) (ISSN: 0976-7312); Volume 10 No. 3, July- September 2015.
- Molotoks, A. H., Doelman Roslyn, Tamas Jonathan, Peter Alexander, Terry Dawson, Pete Smith. N.a. Comparing the impact of future cropland expansion on global biodiversity and carbon storage across models and scenarios. *Philosophical Transactions B*.
- Moran, M., & Jackson, R. (1991). Assessing the Spatial Distribution of Evapotranspiration Using Remotely Sensed Inputs. *Journal Of Environmental Quality*, 20(4), 725-737.
- Naeem, U. A., Gabriel, H. F., Khan, N. M., Ahmad, I., Ur Rehman, H., & Zafar, M. A. (2021). Impact of urbanization on groundwater levels in Rawalpindi City, Pakistan. *Pure and Applied Geophysics*, 178(2), 491-500.
- Neteler, M. (2010). Estimating Daily Land Surface Temperatures in Mountainous Environments by Reconstructed MODIS LST Data. *Remote Sensing*, 2(1), 333-351.
- Ottle, C., & Stoll, M. (1993). Effect of atmospheric absorption and surface emissivity on the determination of land surface temperature from infrared satellite data. *International Journal Of Remote Sensing*, 14(10), 2025-2037.
- Peter H. Gleick. 1993. *Water in Crisis. A Guide to the World's Fresh Water Resources*. Oxford.
- Piero Toscano. Remote sensing application in agriculture. (2020), pg: 871-914.
- Postel, S., Daily, G., & Ehrlich, P. (1996). Human Appropriation of Renewable Fresh Water. *Science*, 271(5250), 785-788.
- Prata, A., Caselles, V., Coll, C., Sobrino, J., & Ottlé, C. (1995). Thermal remote sensing of land surface temperature from satellites: Current status and future prospects. *Remote Sensing Reviews*, 12(3-4), 175-224.
- Priti Attri, Smita Chaudhry, Subrat Sharma. 2015. *Remote Sensing & GIS based Approaches for LULC Change Detection – A Review*.

- Qadir, A., Farooq, A., Khan, T., Zafar, M., & Javed, A. (2019). Water Quality Assessment and Hydrochemistry of Shallow Groundwater in Bhara Kahu area, Islamabad, Pakistan. *International Journal of Economic and Environmental Geology*, 21-25.
- Qamer, F., Shehzad, K., Abbas, S., Murthy, M., Xi, C., Gilani, H., & Bajracharya, B. (2016). Mapping Deforestation and Forest Degradation Patterns in Western Himalaya, Pakistan. *Remote Sensing*, 8(5), 385. MDPI AG.
- Qureshi, Asad & Shah, Tushaar & Akhtar, Mujeeb. (2003). The Groundwater Economy of Pakistan.
- Region, P. M., Rehman, N. U. And Faheem, M. (2022) ‘Modelling of Land Use/Cover and LST Variations by Using GIS and Remote Sensing: A Case Study of the Northern Pakhtunkhwa Mountainous Region, Pakistan’, *Sensors*.
- Romero-Vidal, X. (2019). Two temperatures for one thermostat: The evolution of policy attitudes and support for independence in Catalonia (1991–2018). *Nations And Nationalism*, 26(4), 960-978.
- Sadiq Khan, M., Ullah, S., Sun, T., Rehman, A. U., & Chen, L. (2020). Land-use/land-cover changes and its contribution to urban heat Island: A case study of Islamabad, Pakistan. *Sustainability*, 12(9), 3861.
- Satterthwaite, D. (2009). The implications of population growth and urbanization for climate change. *Environment And Urbanization*, 21(2), 545-567.
- Shannon, h. (2022). Remote sensing applications in gis. Costelloinc.com. Retrieved 18 august 2022.
- Sheikh, I. M., Pasha, M. K., Williams, V. S., Raza, S. Q., & Khan, K. S. (2007). Environmental geology of the Islamabad-Rawalpindi area. *Regional studies of the Potwar plateau area, Northern Pakistan*, 2078, 1.
- Siddique Ullah a, Khalid Ahmad a, Raja Umer Sajjad a, Arshad Mehmood Abbasi a, Abdul Department of Environmental Science’ (no date). ‘Simulating current and future Land Cover Changes and their impacts on Land Surface Temperature in a lower Himalayan region.
- Siebert, S., Kummu, M., Porkka, M., Döll, P., Ramankutty, N., & Scanlon, B. (2015). A global data set of the extent of irrigated land from 1900 to 2005. *Hydrology And Earth System Sciences*, 19(3), 1521-1545.
- Tang, H., & Li, Z. (2013). Land Surface Temperature Retrieval from Thermal Infrared Data. *Quantitative Remote Sensing in Thermal Infrared*, 93-143.
- Tariq, M., & Aziz, R. (2015). An Overview of Deforestation Causes and Its Environmental Hazards in Khyber Pukhtunkhwa. *Core.ac.uk*.
- Thirgood, J. V. 1981. *Man and Mediterranean forest: a history of resources depletion*. Academic Press, 1981.
- Tomlinson, C. J., Chapman, L., Thornes, E., & Baker, C. (2011). Remote sensing land surface temperature for meteorology and climatology: a review. 306, 296–306.
- Tomlinson, C. J., Chapman, L., Thornes, J. E., & Baker, C. (2011). Remote sensing land surface temperature for meteorology and climatology: A review. *Meteorological Applications*, 18(3), 296-306.

- Training samples manager—arcgis pro | documentation. Pro.arcgis.com. (2022). Retrieved 18 August 2022, from <https://pro.arcgis.com/en/pro-app/2.8/help/analysis/image-analyst/training-samples-manager.htm>.
- Tushaar Shah David Molden R. Sakthivadivel and David Seckler. The Global Groundwater Situation: Overview of Opportunities and Challenges. International water management institute. 2000.
- Ullah, S., Tahir, A. A., Akbar, T. A., & Hassan, Q. K., Dewan, A., Khan, A. J., Khan, M., (2019). Remote Sensing-Based Quantification of the Relationships between Land Use Land Cover Changes and Surface Temperature over the Lower Himalayan Region.
- United Nation Framework Convention on Climate Change. 2006. Report on a workshop on reducing emissions from deforestation in developing countries. Twenty-fifth session.
- United Nations. Department of International Economic, United Nations. Department for Economic, Social Information, & Policy Analysis. (1998). World population prospects (Vol. 2). United Nations, Department of International, Economic and Social Affairs.
- University of benin. (2022). Remote sensing and gis [ebook] (2nd ed.). Retrieved 18 august 2022.
- V.L. mcguire, M.R. Johnson, R.L. Schieffer, J.S. Stanton, S.K. Seabee, and I.M. Verstraeten. 2000. Water in Storage and Approaches to Ground-Water Management, High Plains Aquifer. U.S. Geological Survey Circular 1243.
- Vieira, m., formaggio, a., rennó, c., atzberger, c., aguiar, d., & mello, m. (2012). Object based image analysis and data mining applied to a remotely sensed landsat time-series to map sugarcane over large areas. Remote sensing of environment, 123, 553-562.
- Vlahov D, Galea S. Urbanization, urbanicity, and health. J Urban Health. 2002 Dec;79(4 Suppl 1):S1-S12.
- Von Wissmann, H.; Poeh, H.; Smolla, G.; and Kussmaul, F. 1956. On the role of man and nature in changing the face of the dry belt of Asia.
- Vorobyova, T., & Smagulov, Y. (2021). Mapping dynamics of agricultural land use in the dry steppe zone of the Northern Kazakhstan. Intercarto. Intergis, 27(4), 5-18.
- Wan, Z. And Dozier, J. (1996) A Generalized Split-Window Algorithm for Retrieving Land-Surface Temperature from Space. IEEE Transactions on Geoscience and Remote Sensing, 34, 892-905.
- Weng, Q. (2003). Fractal Analysis of Satellite-Detected Urban Heat Island Effect. Photogrammetric Engineering & Remote Sensing, 69(5), 555-566.
- What is a mosaic? Arcmap | documentation. Desktop.arcgis.com. (2022). Retrieved 18 August 2022, from <https://desktop.arcgis.com/en/arcmap/latest/manage-data/raster-and-images/what-is-a-mosaic.htm>.
- William A. Jury, Henry J. Vaux, The Emerging Global Water Crisis: Managing Scarcity and Conflict Between Water Users, Advances in Agronomy, Academic Press, Volume 95, 2007, Pages 1-76, ISSN 0065-2113, ISBN 9780123741653.
- William L. Thomas. 1956. Man's role in changing the face of the earth. The University of Chicago; Chicago Illinois; 1956.

- Yan, H., Liu, J., Huang, H., Tao, B., & Cao, M. (2009). Assessing the consequence of land use change on agricultural productivity in China. *Global And Planetary Change*, 67(1-2), 13-19.
- Yann H. Kerr, Jean Pierre Lagouarde, Françoise Nerry, Catherine Ottlé. Land surface temperature retrieval techniques and applications. CRC Press. 2004.

Appendices

Appendix 1

Classified	Vegetation	Barren	Forest	Water	Urban	Total
Vegetation	12	6	5	0	0	23
Barren	41	36	0	13	11	101
Forest	1	0	49	2	0	52
Water	0	0	0	32	0	32
Urban	2	11	0	3	43	59
Total Classified Points	56	53	54	50	54	267
Total Corrected Reference Points	172					
Total True Reference Points	267					
Percent Accuracy	70.42					
User Accuracy			Producer's Accuracy			
Vegetation	52.17		Vegetation	21.43		
Barren	35.64		Barren	67.92		
Forest	94.23		Forest	90.74		
Water	100.00		Water	64.00		
Urban	72.88		Urban	79.63		
Total	71.99		Total	71.74		

Appendix 2

Classified	Water	Vegetation	Forest	Barren	Urban	Total
Water	39	1	0	0	0	40
Vegetation	6	16	2	7	0	31
Forest	0	2	50	0	0	52
Barren	2	27	0	45	5	79
Urbanization	4	9	0	4	51	68
Total Classified Points	51	55	52	56	56	270
Total Correct Reference Points	201					
Total True Reference Points	270					
Percent Accuracy	74.44					

User's Accuracy			Producer's Accuracy			
Water	97.5		Water	76.47		
Vegetation	51.61		Vegetation	29.09		
Forest	96.15		Forest	96.15		
Barren	56.96		Barren	80.36		
Urbanization	75		Urban	91.07		
Total	75.45		Total	76.63		

Appendix 3

Classified	Vegetation	Barren	Settlement	Water	Forest	Total
Vegetation	13	7	2	1	2	25
Barren	26	45	0	6	0	77
Settlement	8	0	80	13	0	101
Water	0	0	0	44	0	44
Forest	8	0	3	19	51	81
Total Classified Points	55	52	85	83	53	328
Total Correct Reference Points	233					
Total True Reference Points	328					
Percent Accuracy	71.04					
User's Accuracy			Producer's Accuracy			
Vegetation	52.00		Vegetation	23.64		
Barren	58.44		Barren	86.54		
Settlement	79.21		Settlement	94.12		
Water	100.00		Water	53.01		
Forest	62.96		Forest	96.23		
Total	70.52		Total	70.71		

Appendix 4

Classified	Water	Barren	Vegetation	Forest	Urban	Total
Water	47	0	1	0	0	48
Barren	5	61	21	0	1	88
Vegetation	1	5	22	1	0	29
Forest	0	0	3	53	0	56
Settlement	0	0	5	0	53	58
Total Classified Points	53	66	52	54	54	279
Total Correct Reference Points	236					
Total True Reference Points	279					
Percent Accuracy	84.59					
User's Accuracy			Producer's Accuracy			
Water	97.92		Water	88.68		
Barren	69.32		Barren	92.42		
Vegetation	75.86		Vegetation	42.31		
Forest	94.64		Forest	98.15		
Urban	91.38		Urban	98.15		
Total	85.82		Total	83.94		

ASSESSMENT OF LULC AND LST OF ISLAMABAD AND RAWALPINDI,

ORIGINALITY REPORT

3 %	3 %	2 %	0 %
SIMILARITY INDEX	INTERNET SOURCES	PUBLICATIONS	STUDENT PAPERS

PRIMARY SOURCES

1	arset.gsfc.nasa.gov Internet Source	1 %
2	www.rjgeo.ro Internet Source	1 %
3	m.scirp.org Internet Source	1 %
4	www.mdpi.com Internet Source	1 %

Exclude quotes ☒ On
Exclude bibliography ☒ On

Exclude matches ☒ < 1%